Available online at www.sciencedirect.com
ScienceDirect
Trans. Nonferrous Met. Soc. China 34(2024) 3069−3092
Transactions of Nonferrous Metals Society of China
www.tnmsc.cn

Microstructural evolution and deformation mechanisms of superplastic aluminium alloys: A review

Guo-tong ZOU[1], Shi-jie CHEN[1], Ya-qi XU[1], Bao-kun SHEN[1], Yu-jia ZHANG[1], Ling-ying YE[1,2,3]

1. School of Materials Science and Engineering, Central South University, Changsha 410083, China;
2. Key Laboratory of Nonferrous Metal Materials Sciences and Engineering, Ministry of Education, Central South University, Changsha 410083, China;
3. Nonferrous Metal Oriented Advanced Structural Materials and Manufacturing Cooperative Innovation Centre, Central South University, Changsha 410083, China

Received 30 June 2024; accepted 26 September 2024

Abstract: Aluminium alloy is one of the earliest and most widely used superplastic materials. The objective of this work is to review the scientific advances in superplastic Al alloys. Particularly, the emphasis is placed on the microstructural evolution and deformation mechanisms of Al alloys during superplastic deformation. The evolution of grain structure, texture, secondary phase, and cavities during superplastic flow in typical superplastic Al alloys is discussed in detail. The quantitative evaluation of different deformation mechanisms based on the focus ion beam (FIB)-assisted surface study provides new insights into the superplasticity of Al alloys. The main features, such as grain boundary sliding, intragranular dislocation slip, and diffusion creep can be observed intuitively and analyzed quantitatively. This study provides some reference for the research of superplastic deformation mechanism and the development of superplastic Al alloys.

Key words: aluminium alloys; superplasticity; superplastic deformation mechanism; grain boundary sliding; microstructural evolution

1 Introduction

Superplasticity is the special property of polycrystalline materials that show an elongation of hundreds of percent at relatively high temperatures (>0.5T_m; T_m is the melting point) and low strain rates (10^{-4}−10^{-1} s^{-1}) [1−3]. The technology of component manufacturing utilizing the superplasticity of materials is called superplastic forming (SPF), which helps to achieve near-net-shape manufacturing of large parts [4−6]. The elongation of superplastic Al alloys can vary from 200% to 2000%, and the equivalent thickness strains achieved in Al alloys can exceed 300% during SPF [6]. the combination of Al alloys and SPF technology, with the advantages of high efficiency, low cost and lightweight, is widely used now and expected to grow rapidly in the future [4,7].

Typically, for Al alloys, to achieve superplasticity, a fine grain structure with an average grain size below 10 μm is needed [8]. Some processing technologies such as thermomechanical processing (TMP) [9−27], high-pressure torsion (HPT) [26−36], friction stir processing (FSP) [37−63], equal-channel angular pressing (ECAP) [64−96], etc. have been developed to refine the grains of Al alloys. Among these process technologies, TMP is most widely used in producing superplastic Al alloys due to its cost advantages and ability to obtain large-sized sheets. The process technologies of FSP, HPT, ECAP, etc. are classified into severe

Corresponding author: Ling-ying YE, Tel: +86-13607435545, E-mail: lingyingye@csu.edu.cn
DOI: 10.1016/S1003-6326(24)66596-9

plastic deformation (SPD). According to the initial grain structure prior to deformation, superplastic Al alloys can be divided into two types: one is with initial banded structure and the other is with fine equiaxed grains [8], and the initial grain structure is mainly determined by the elemental composition and processing method.

With the research in the past decades, researchers have gradually established a theoretical system of superplastic deformation mechanisms with grain boundary sliding (GBS), diffusion creep (DC), and intragranular dislocation slip (IDS) as the main deformation mechanisms. Some classical superplastic deformation mechanisms such as Ball−Hutchison model [97], Ashby−Verrall model [98], and Core−mantle model [99] have been proposed and widely accepted. Moreover, some new technologies such as high-resolution electron backscatter diffraction (EBSD) [65,66], focus ion beam (FIB) [25,100,101], in-situ scanning electron microscopy (SEM) [25,102,103] have been carried out to investigate the superplasticity of Al alloys and have obtained some new insights. During superplastic deformation or SPF, due to the combination of elevated temperature and large strain, Al alloys would experience sever micro-structure evolution. Furthermore, due to the difference of initial grain structure, Al alloys show different superplastic deformation behaviours and mechanisms. Better understanding of the micro-structure evolution and deformation mechanism of Al alloys during superplastic deformation is vital for selecting optimal forming parameters and service performances.

In this work, the recent development and research focus in superplastic Al alloys are summarized. The development and application history of superplastic Al alloys are retrospectively reviewed, and their research status is analyzed comprehensively. In addition, the microstructure evolution of Al alloys during superplastic deformation is summarized and analyzed. The typical cases of superplasticity research in Al alloy by using mechanical behaviour analysis are summarised. The newly developed method for quantitative research of superplastic deformation mechanism, the FIB-assisted surface study, is introduced and discussed. Finally, the future research focus and development direction of superplastic Al alloy are introduced.

2 History and application background of superplastic Al alloys

Recognized research on superplasticity began in 1934 when PEARSON [104] discovered a tensile elongation of 1950% in Pb−Sn eutectic alloy. Since then, superplasticity has been developed in various materials, especially in Al alloys. In 1964, BACKOFEN [105] published a landmark paper reporting the pneumatically formed “bubble” of superplastic Al−Zn eutectic alloys, unlocking the prelude to the development of superplastic forming. Based on the technologies in the field of superplastic Al alloys (especially Al−6wt.%Cu−0.5wt.%Zr alloy), the first SPF company, Superform Metals, was established in England in 1973 [4]. The superplastic Al−6%Cu−0.5%Zr alloy, called SUPRAL 100, has achieved great commercial success since then.

In the late 1970s, due to the impact of rising global oil prices, superplastic Al alloys were rapidly developed and widely used in the aviation field. The high-strength Al alloys such as AA7475 alloy, Al−Cu−Mg alloy, and Al−Li−Zr alloy were developed during that period. These alloys can be classified into the second-generation superplastic Al alloys [5,6], by adding trace elements such as Sc and Zr, to achieve grain refinement and prevent grain growth. Most of the second-generation superplastic Al alloys were prepared by TMP and mainly used in the aerospace, automotive, rail, and architecture fields [4]. In 1992, Boeing first used SPF to manufacture the blowout door assembly on the 737 with superplastic 7475 alloy [106]. In around 2000, General Motors Company (GM) creatively improved the SPF technology and extended it to the auto industry, and the representative application is the manufacturing of liftgates by using superplastic 5083 alloy [4]. A lot of interests produced by SPF of Al alloys such as building panels, unconventional chairs, frame of bicycles came out in that period [107].

The rapidly developed SPD technology spawned the development of the third generation of superplastic Al alloys [5,6,108,109]. By using SPD, ultrafine-grained structures [29,30,43,45,75] and even nanocrystalline structures [33,35] can be introduced into Al alloys, and these alloys are more likely to exhibit low-temperature and/or high-strain-

rate superplasticity. Although Al alloy has become widely used superplastic materials due to its lower production cost, earlier application and higher comprehensive properties, its application is now suffering from the challenges of other superplastic alloys, such as lighter magnesium alloys [3,110], higher strength titanium alloys [111−113], and even high entropy alloys [114,115]. Researchers and manufacturers are recommended to develop more competitive superplastic Al alloys such as those with low-temperature superplasticity and high-strain-rate superplasticity, while reducing the manufacturing cost and improving their service performance, to further enhance the competition of superplastic Al alloys.

3 Research status of superplastic Al alloys

The number of published research papers on superplastic Al alloys as a function of year is counted and shown in Fig. 1. According to Fig. 1, before 1999, the publications on superplastic Al alloys were not much. From 1999 to the beginning of the 21st century, the research on superplastic Al alloys ushered in explosive growth, which can be attributed to the development of SPD technologies. Since 2010, the number of papers published on the superplasticity of Al alloy has remained at a stable level, which indicates that this field has been a research hotspot.

Figure 2 shows the quantities of papers related to superplastic Al alloys published by each country or region from 2000. More than 20 countries or regions in the world have conducted research on the superplasticity of Al alloys, of which China accounts for the largest number of papers published, followed by Russia and USA.

The main brand of superplastic Al alloys, their processing methods, and the grain structure prior to deformation are shown in Fig. 3. The most studied brand of superplastic Al alloys is Al−Mg-based (5xxx) alloy, accounting for ~45%, followed by Al−Zn−Mg−Cu (7xxx) alloys (~28%) and Al−Cu-based (2xxx) alloys (~10%). Superplasticity has also been reported in other grades of Al alloys such as Al−Si alloy, Al−Li alloy, and pure Al. For the processing methods, TMP is most widely used to produce superplastic Al alloys accounting for ~44%, and the proportion of ECAP and FSP is almost the same, accounting for ~20%, respectively. HPT accounts for 6% and some other methods such as extrusion and cross-rolling account for ~10%. The grain structure of Al alloys before superplastic deformation can be divided into two types: equiaxed and banded (or called recrystallized and unrecrystallized). According to Fig. 3, banded-grained superplastic Al alloys are mainly produced by TMP. The SPD methods containing ECAP, FSP, and HPT generally introduce fine, equiaxed grains into superplastic Al alloys.

4 Microstructure evolution in Al alloys during superplastic deformation

In general, there are two microstructural prerequisites for superplastic materials to obtain considerable elongation: (1) fine equiaxed grain structure so as to provide high density of grain boundaries and then motivate GBS; (2) fine grain structure that can remain stable under the combination of high temperature and high stress [5]. For Al alloys, fine equiaxed grain structure can be

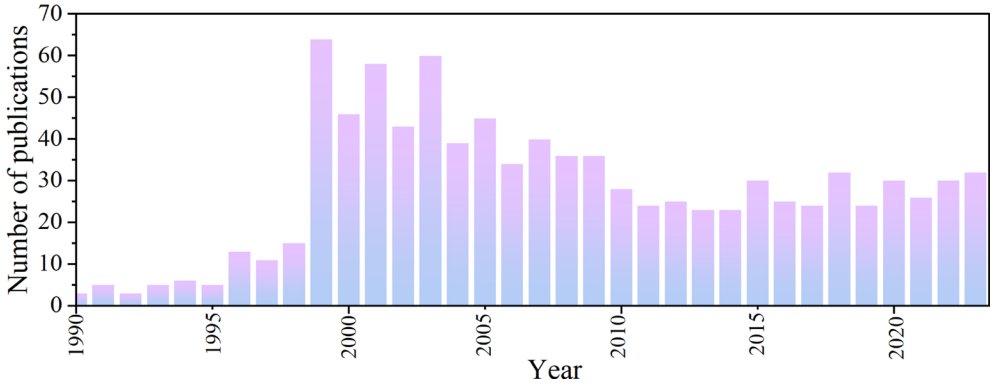

Fig. 1 Number of published research papers on superplastic Al alloys as function of year

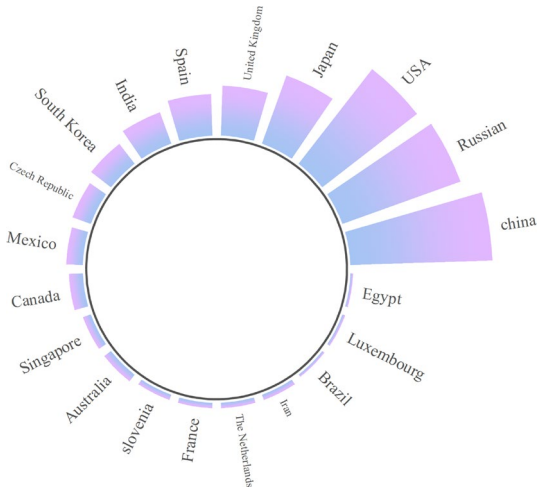

Fig. 2 Ring bar chart showing contribution of each country or region to published papers related to superplastic Al alloys from 2000

obtained by static recrystallization or by dynamic recrystallization during hot deformation. The rules of microstructure evolution of these two types of superplastic Al alloys are different [25,100]. Furthermore, during superplastic deformation, microstructures such as texture, cavity, and secondary phase would evolve strongly [10]. Understanding the microstructure evolution of Al alloys during superplastic deformation is of great significance in regulating the microstructures and properties of parts after SPF.

4.1 Grain structure evolution of Al alloys with initial unrecrystallized structure during superplastic deformation

For Al alloys with initial unrecrystallized structure, during superplastic deformation, fine approximately-equiaxed grain structure can be obtained via dynamic recovery and dynamic recrystallization [59]. Typically, the structure of these Al alloys is stabilized against static recrystallization by Sc or Zr dispersoids [8,59]. When conducting superplastic deformation to these rolled or extruded Al alloys, the process of banded grains evolving into equiaxed shape dynamically plays a vital role in the whole deformation stage.

ZHANG et al [13] compared the high-temperature tensile properties of Al−Mg−Sc−Zr alloys with different Sc/Zr ratios and found that the alloy with a higher Sc/Zr ratio can achieve much larger elongation. This is because the combination effects of discontinuous dynamic recrystallization (DDRX) and pinning force from Al_3Sc precipitates result in homogeneous fine equiaxed grains during deformation, which facilitates the GBS at the subsequent deformation stage. When investigating the hot deformation of Al−Cu−Zr alloys, SOTOUDEH and BATE [100] noticed that superplasticity was found in alloys with high solute content. By comparing the grain structure after deformation, it was found that in Al−2Cu−Zr alloy, the grain remained a banded shape after tensile deformation, and oppositely, Al−4Cu−Zr alloy exhibited an equiaxed shape after deformation. This further proves the importance of fine equiaxed grain structure to the superplastic Al alloy.

LIU et al [59] analysed the microstructure evolution process of a band-grained Al−Mg−Sc alloy during superplastic deformation and divided it into three stages: sub-grain rotation and coalescence at the early stage, dynamic recrystallization at the middle stage, and GBS and grain growth at the final

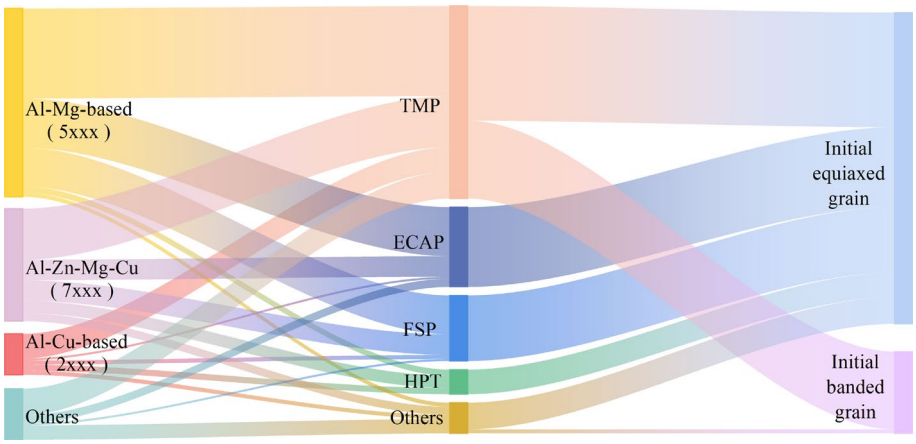

Fig. 3 Sankey diagram showing proportion and relationship of superplastic Al alloys, producing process, and initial grain structures

stage. The grains transformed into equiaxed shape at the true strain of 1.6 and then this microstructure with random distribution was kept until fracture. Figure 4 shows the typical grain structure evolution process of 5A90 alloy during superplastic deformation [116]. It can be seen that the banded grains transform into equiaxed shape gradually with the increase of superplastic strain.

ZOU et al [25] investigated the grain structure evolution of a band-grained 2A97 Al−Cu−Li alloy during superplastic deformation systematically. This alloy shows an excellent elongation (525%) when stretched at 430 °C and 2×10^{-3} s^{-1}. As can be seen in Fig. 5, with the true strain increases from 0.35 to 1.1, the banded grains are replaced by equiaxed grains; when the true strain continues to increase to 1.6, the dynamically generated equiaxed grains grow and extend along the tension direction. By quantitative analysis, with the increase of true strain from 0.35 to 1.6, the fraction of low angle

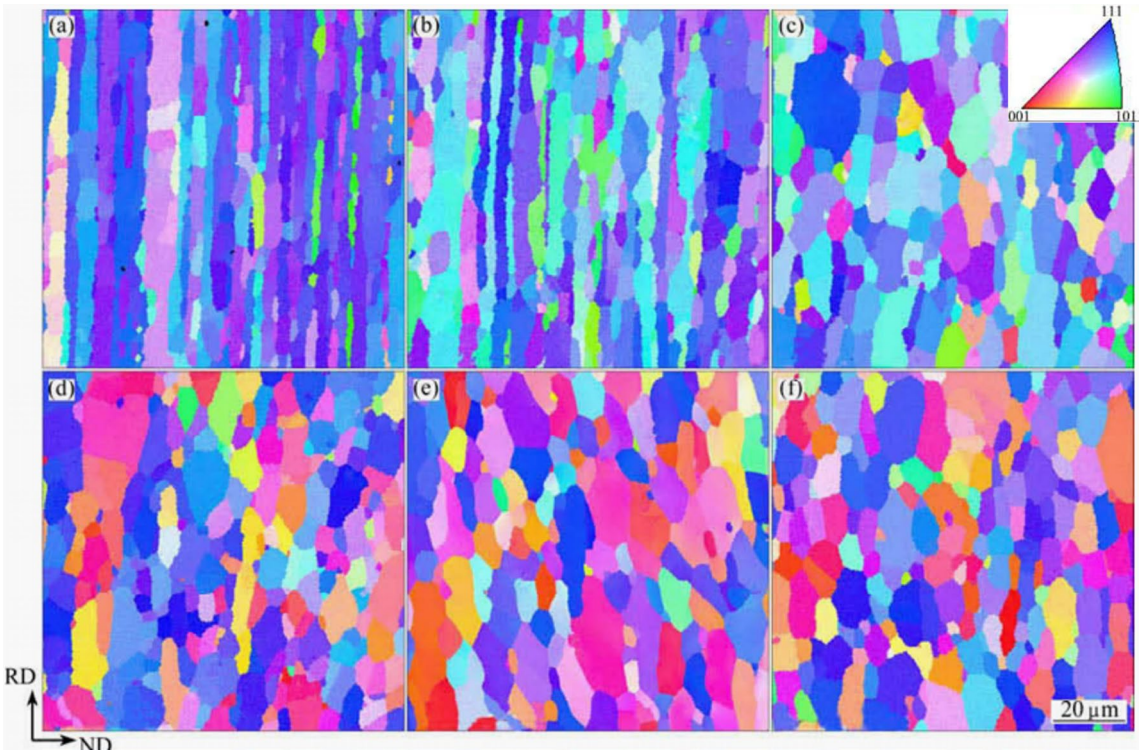

Fig. 4 EBSD images of 5A90 alloy after being stretched to different true strains [116]: (a) 0.18; (b) 0.5; (c) 0.56; (d) 0.9; (e) 1.16; (f) 1.27

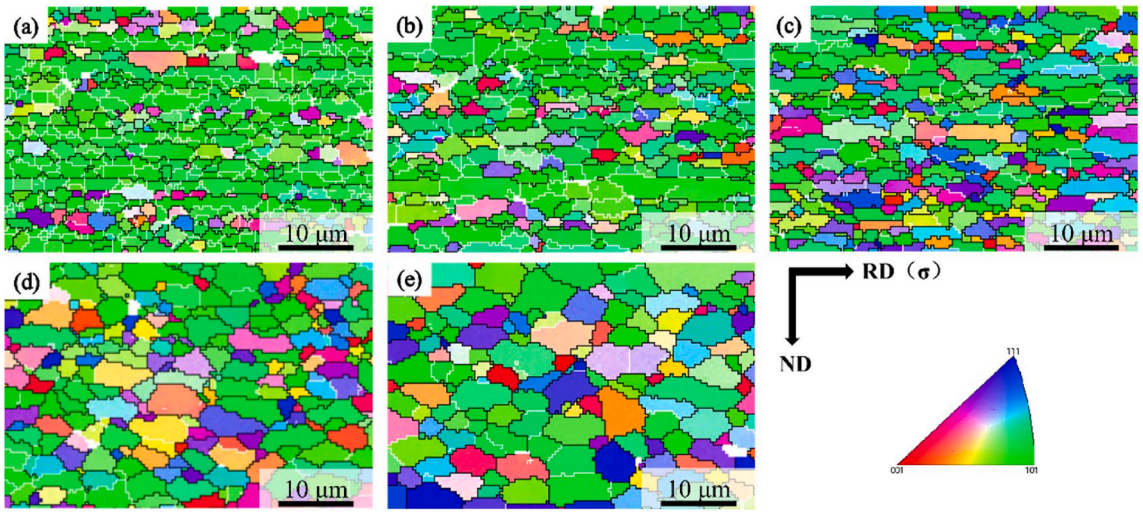

Fig. 5 IPF maps of 2A97 Al−Cu−Li alloy after being superplastically deformed to different true strains [25]: (a) 0.35; (b) 0.7; (c) 1.1; (d) 1.4; (e) 1.6

grain boundaries decreases from 29.5% at the true strain of 0.35 to 7.8%, which indicates that the CDRX occurs and results in grain evolution.

4.2 Grain structure evolution of Al alloys with initial recrystallized structure during superplastic deformation

The Al alloys with fine equiaxed grains prior to superplastic deformation are mainly produced by SPD [59,66,82,117] or via recrystallized annealing after TMP [28,103]. The grain structure evolution in these superplastic Al alloys is relatively stable and is related to their deformation mechanisms. When the superplastic deformation mechanism is dominant by GBS, the grains would remain nearly equiaxed shape with random grain misorientations until large strain and even after fracture, which is caused by the competition between GBS and grain growth [59,103]. In other works [65,66], dynamic recrystallization was observed during deformation in initial fine-grained superplastic Al alloys. This is because the elongated grains are subdivided into chains of fine grains via continuous dynamic recrystallization (CDRX) [65].

Based on EBSD results and previous research works [118], LIU et al [59] proposed a schematic microstructure evolution mechanism combining GBS and grain growth. Significant GBS occurs between the fine and equiaxed grains and then results in random grain rotation. The HAGBs and LAGBs convert to each other due to the random grain rotation. Grain growth and grain shape change act as accommodating role during the superplastic deformation to avoid cavitation. MASUDA et al [119] found that the grain grew more rapidly in the tensile direction in a fine-grained Al−Mg−Mn alloy after superplastic deformation, and they proposed a mechanism of dynamic anisotropic grain growth by using EBSD and surface study: neighbouring grains rotate and coalesce with each other due to GBS, resulting in the grain size growth along the tensile direction.

Figure 6 shows the grain structure evolution of a fine-grained Al−Cu−Li alloy during superplastic deformation [103]. Before superplastic deformation, the tested alloy had nearly equiaxed grains with an average grain size of (6.7±0.6) μm. After being stretched to fracture at 490 °C and 2×10^{-4} s^{-1}, the grains near the fracture area grew up to (20.3±2.1) μm. The grains at the undeformed grip section kept a stable status, with an average grain size of (8.5±0.9) μm. The microstructure evolution

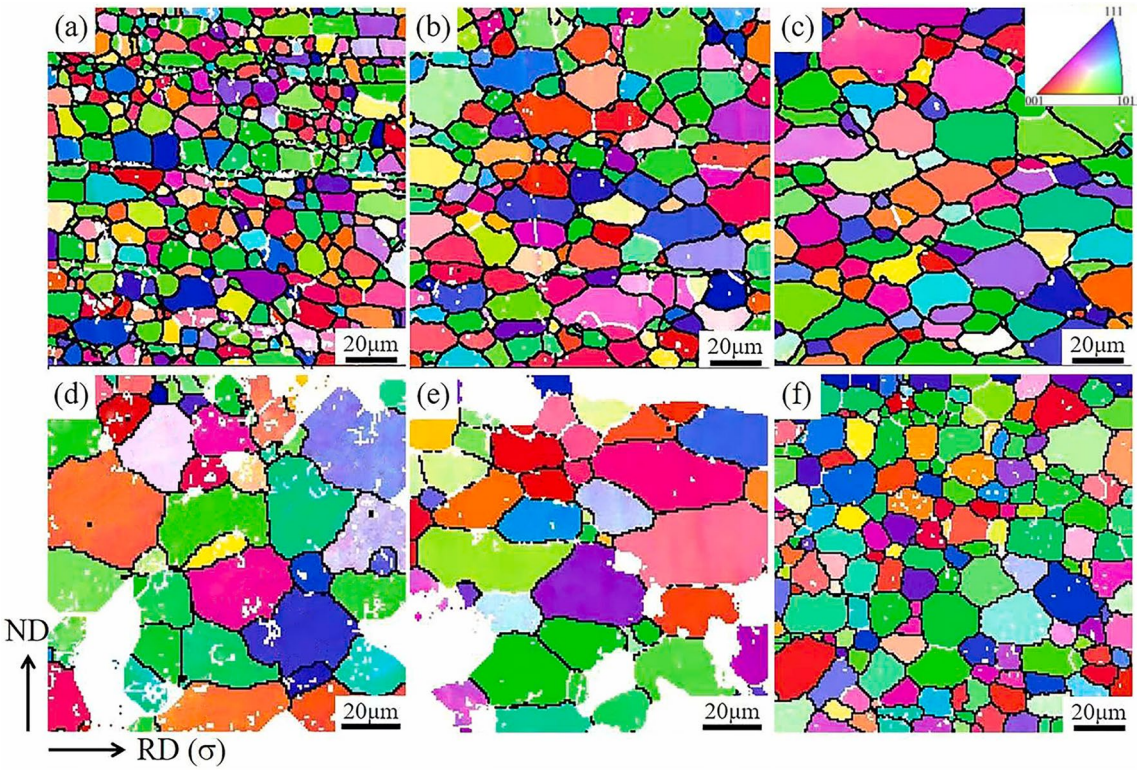

Fig. 6 EBSD IPF maps of fine-grained Al−Cu−Li alloy deformed to different true strains [103]: (a) 0; (b) 0.69; (c) 1.2; (d) 1.79; (e) 2.01; (f) Grip section

was divided into three stages: during the strain range of 0.1−1.2, the grains remained nearly equiaxed and the flow curve was stable; after this stage, dynamic recrystallization occurred and resulted in strain softening; with the strain continued to increase, rapid grain growth could be observed, which resulted in strain hardening.

SONG et al [29] investigated the room-temperature superplasticity of an ultrafine-grained Al−Zn alloy and observed its grain evolution process by using in-situ EBSD. The in-situ evolution process of grains is shown in Fig. 7. The Grains A, B, and C, which were initially vertically aligned, gradually evolved to be horizontally aligned at the strain of 115%. After that, with increasing the strain, the three grains separated from each other. The change in IPF colour of Grain A demonstrated its rotation. After being deformed to the stain of 200%, these grains kept equiaxed shape and the average grain size was found to have no noticeable change. The above analysis proves that the superplastic deformation of the studied alloy is governed by GBS and grain rotation.

4.3 Evolution of texture, secondary phase, and cavitation in superplastic Al alloy

(1) Texture

The texture evolution of Al alloys during superplastic deformation is a common phenomenon accompanied by the grain structure evolution, especially for those Al alloys with initial banded grains [8,10,59,116]. Some researchers [13,59,120] proposed that if sub-grain growth develops rapidly during superplastic deformation, the texture will maintain its initial structure or slightly weaken with increasing strain because the HAGBs are developed from grain boundary migration. This process is now called discontinuous dynamic recrystallization (DDRX). On the contrary, if the recrystallization is dominant by sub-grain rotation assisted by sliding behaviour, the texture will become diffused gradually or even be randomly distributed [10,121]. This process is now called continuous dynamic recrystallization (CDRX).

During the superplastic deformation, dynamic recrystallization would result in texture spreading and randomization [8,10,59,116]. ZOU et al [10] investigated the evolution of macrotextures of an initial banded superplastic Al alloy by using X-ray diffraction (XRD), as shown in Fig. 8, where the maximum texture strength is reduced, which proves the spreading of texture. Furthermore, from the quantitative results given in Fig. 9, it can be observed that the rolling textures (Brass, S, and Cupper) weaken with the increase of superplastic strain, and the recrystallization textures (Goss and Cube) grow. This process is attributed to the recrystallization process induced by the particle stimulated nucleation (PSN) during superplastic deformation.

(2) Secondary phases

Like other high-temperature deformations, superplastic deformation would result in changes in secondary phases due to elevated temperature and strain. As mentioned in Section 4.1, Sc or Zr element is often added into Al alloys to stabilize the grain size and inhibit recrystallization; furthermore, adding Sc or Zr would increase the strain rate

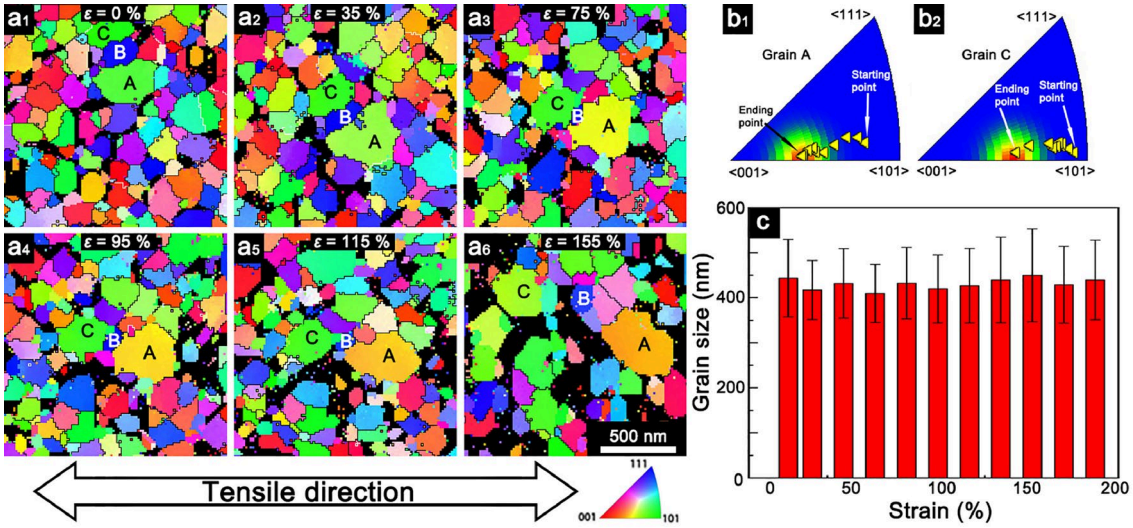

Fig. 7 EBSD maps of Al−Zn alloy at different strains by using in-situ observation [29]

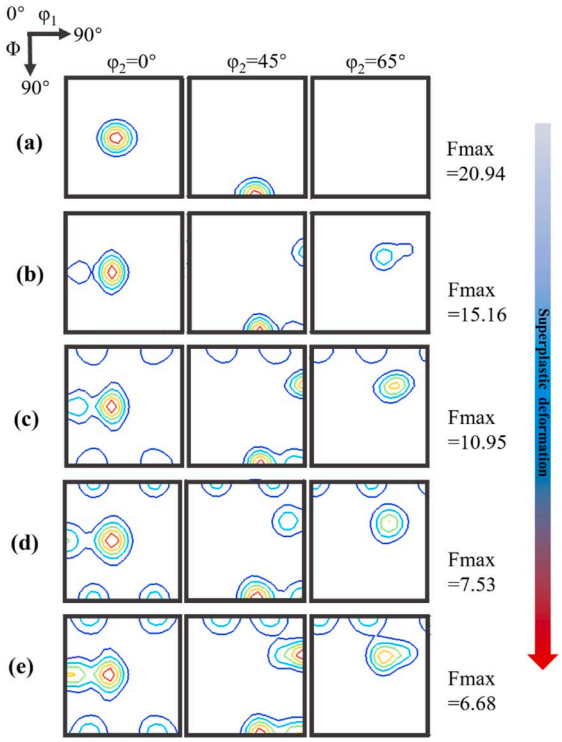

Fig. 8 ODF sections of superplastic 2A97 Al−Cu−Li alloy after being deformed to different strains [10]: (a) 0; (b) 50%; (c) 100%; (d) 150%; (e) 200%

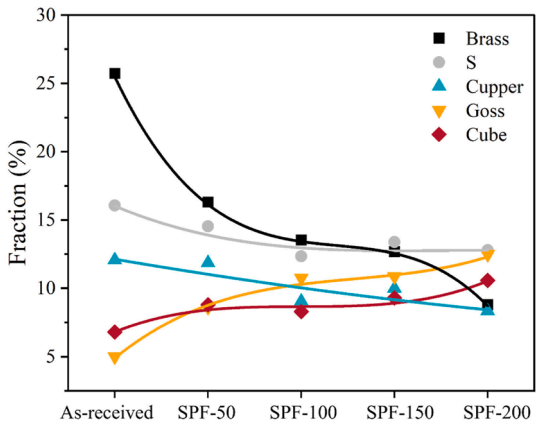

Fig. 9 Fraction of main texture components of superplastic 2A97 Al−Cu−Li alloy after being deformed to different strains [10]

sensitivity (m) and decrease the deformation activation energy (Q) [122]. The Sc or Zr element tends to precipitate as $L1_2$-structured Al_3X nanoscale precipitates (dispersoids) during the homogenization treatment [41,123,124]. The initial structure of these dispersoids and their evolution during superplastic deformation have a significant influence on superplasticity. DENG et al [122] investigated the evolution of $Al_3(Sc_{1-x}Zr_x)$ in Al−Zn−Mg alloys. They found that after superplastic deformation (deformation parameters: 500 °C, 0.01 s^{-1}), the size of $Al_3(Sc_{1-x}Zr_x)$ particles increased from (9.8±3.4) nm to (16.4±6.8) nm, their number density decreased, and the lattice misfit between particle and Al matrix increased from 1.04% to 1.30%.

Apart from the $L1_2$-structured Al_3X nanoscale precipitates, coarse secondary phases generated by high temperature over-ageing are often introduced into Al alloys, especially for those Al alloys produced by TMP [23,25,125]. These large-sized phases can act as nucleation sites during static annealing or hot deformation and then refine the grains, which is called "particle-stimulated nucleation" (PSN) [126,127]. ZOU et al [10] found that with increasing the strain, the volume fraction of coarse secondary phases decreased gradually; however, those phases larger than 0.8 μm increased. By conducting an in-situ SEM, as shown in Fig. 10, the coarsening and dissolution of phases were noticed simultaneously, which can be attributed to the diffusion of solute atoms [128,129]. WANG et al [9] investigated the phase evolution of a superplastic 2198-T8 Al−Cu−Li alloy at different deformation temperatures (400−550 °C). They found that T_1 phases disappeared when deformed at temperatures higher than 450 °C, and S' phases coarsened with increasing the temperature.

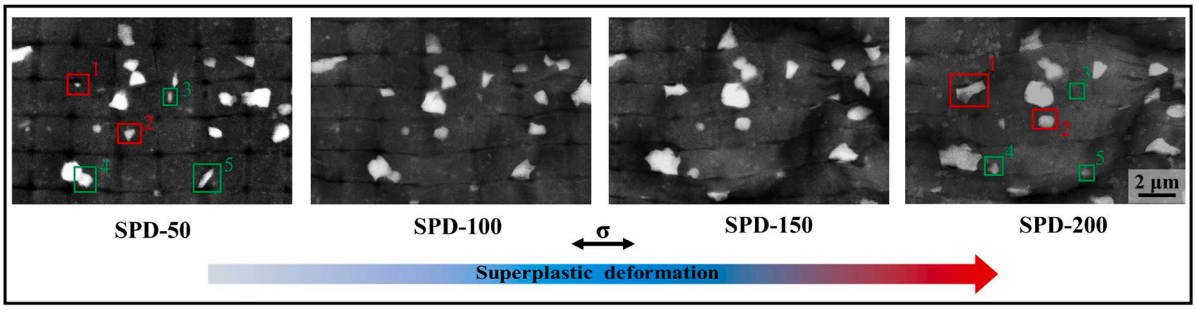

Fig. 10 Evolution of coarse secondary phases during superplastic deformation [10]

(3) Cavitation

Cavities have an adverse influence on the properties of Al alloys, and most superplastic materials fail due to the nucleation, growth, and interlinkage of cavities during superplastic deformation [130]. CHOKSHI [130] pointed out that the nucleation of cavities in superplastic materials can be attributed to stress concentration. The stress concentrations are likely to develop around the sites of triple junctions, grain boundary ledges, and grain boundary particles due to GBS [131]. Several mathematical models of superplastic cavity initiation were given [130]. As shown in Fig. 11, the cavity formation mechanism indicates that the nucleation of the cavity is caused by the mismatch between dislocation slip and dislocation climb at the grain boundary [132]. According to the research conducted by BAE and GHOSH [133], most cavities initiated and grew at the interface between matrix and particles, and the cavity fraction increased with increasing the strain rate and decreasing the deformation temperature. ZOU et al [10] recorded the process of cavitation in an Al−Cu−Li alloy during superplastic deformation and found that the cavities initiated from the triple junctions and then grew with GBS and grain rotation, and these cavities resulted in the decrease of ductility of material after the superplastic deformation.

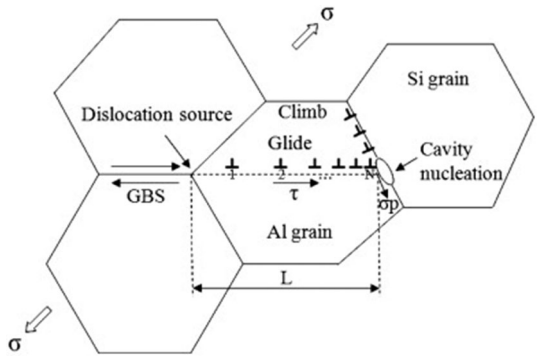

Fig. 11 Mechanism of cavity formation for Al−Si−Mg alloy during superplastic deformation [132]

5 Superplastic deformation mechanism research based on deformation behaviour analysis

Superplasticity can be divided into three regions according to the flow behaviour: Region I, Region II, and Region III with low, high, and again low m values, respectively [1,134]. The GBS is activated and even plays the dominant role in superplastic Region II [1,134], and most of the superplastic Al alloys are in this region. When Region II transits into Region III with increasing the strain rate and/or decreasing the temperature, the m value decreases to ~0.2 and intragranular dislocation climb occurs. Strain rate sensitivity (m) is an important index for superplastic materials and even determines the elongation, and materials with high m value usually show good resistance to necking behaviour [2,6]. Typically, the m value can be obtained by using the constant strain rate method [135] and the strain rate jump method [105].

In the constant strain rate method [135], a series of uniaxial tensile tests are carried out under constant strain rate conditions, and then the stress−strain curves are obtained. By drawing the plots of the naturally logarithmic relationship between stress and strain rate under a particular level of strain, the m value can be obtained according to the formula:

$$m=\partial \ln \sigma / \partial \ln \dot{\varepsilon} \tag{1}$$

where σ is the stress and $\dot{\varepsilon}$ is the strain rate.

The strain rate jump method [105] is also conducted under uniaxial tensile conditions. The stretching is started at a strain rate; after a certain interval of strain, strain rate is increased (usually by 10%−25%) and kept for the same interval, and then restored to the initial strain rate. In a test, it is usually to set multiple strain rate jump intervals to obtain the stress change values at different strain stages. The m value can be obtained with the following formula:

$$P=A_0\sigma e^{-\varepsilon} \tag{2}$$

$$m=\frac{\ln(P_2/P_1)}{\ln(\dot{\varepsilon}_2/\dot{\varepsilon}_1)} \tag{3}$$

where P is the load applied, A_0 is the original area, ε is strain, and P_1 and P_2 are the loads on both sides of the jumped curve.

The typical m values obtained by using the constant strain rate method and the strain rate jump method are demonstrated in Figs. 12(a, b), respectively. In many works [12,13,20,125,136], m value was calculated to understand or predict the superplastic deformation mechanism of Al alloys. YAKOVTSEVA et al [136] measured the m values in an Al−Mg-based alloy during superplastic

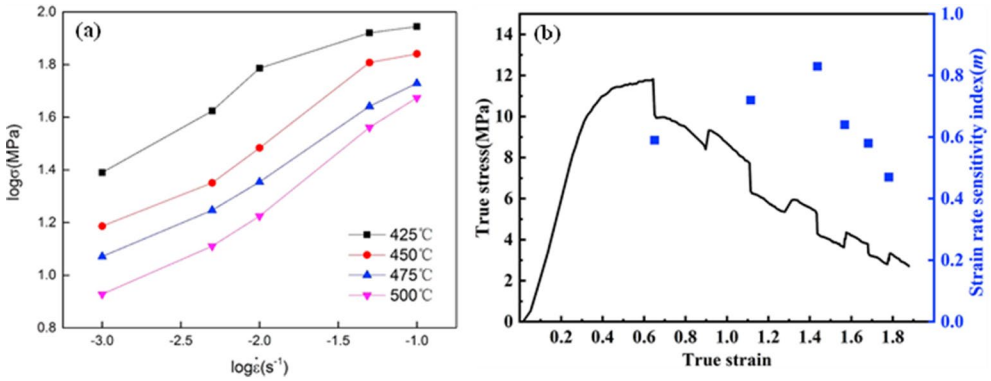

Fig. 12 Measured *m* values by using the constant strain rate method [15] (a), and strain rate jump method showing *m* value changes with increasing strain [125] (b)

deformation by using the strain rate jump method, and they found that despite the presence of dynamic recrystallization, the measured *m* value did not change significantly with the change of strain rate and increasing strain. This is because the grains transformed into an equiaxed shape quickly and the dynamic grain growth was insignificant. The GBS played a dominant role and even provided a contribution up to 41% to the total strain. However, a decrease of *m* value from 0.6 to 0.4 with increasing strain was noticed in fine-grained Al−Mg-based alloys, because the significant dynamic grain growth and grain elongation during superplastic deformation resulted in a weaker GBS [20]. GHAYOUMABADI et al [12] compared the *m* values of AA6013 alloys with different Y, Sc, and Zr additions by using the constant strain rate method. It was found that the *m* value for the alloy with minor additions was higher because the trace elements refined the grains and facilitated GBS.

ZOU et al [25] obtained the *m* values of a 2A97 Al−Cu−Li alloy with the strain rate jump method and noticed that the *m* value increased from ~0.4 to ~0.5 from the initial deformation stage to the middle stage and then decreased to ~0.4 again with further increasing strain. By analyzing the microstructure evolution, the authors found that the grain structure and deformation mechanism significantly affected the measured *m* value. In the primary deformation stage, the alloy had banded grain structure, and the main deformation mechanism was IDS; with the increase of strain, the grain structure transformed to an equiaxed shape and GBS became the dominant deformation mechanism, so the *m* increased; when the strain increased continuously, the grains grew and then the *m* value of the alloy decreased. The same variation of m values was reported by LIU et al [125].

The above cases prove intrinsic relationship between *m* value and superplastic deformation mechanism, and show the importance of GBS in superplastic Al alloys. Apart from *m*, the activation energy (*Q*) can also be used to analyze and predict the superplastic deformation mechanism [2]. The *Q* of Al alloys for hot deformation represents mainly the free energy barrier to dislocation slipping on slip planes. In Al alloys, *Q* (=84 kJ/mol) is the grain boundary diffusion coefficient and is considered to indicate the mechanism of GBS; the *Q* value of lattice diffusion is 142 kJ/mol and corresponding deformation mechanism is expected to be solute drag creep [2,137]. The *Q* value can be obtained by using the following equation:

$$Q = \frac{R}{m}\frac{\partial \ln \sigma}{\partial (1/T)}\Big|_{\dot{\varepsilon}} \tag{4}$$

where *R* is the molar gas constant, and *T* is the deformation temperature.

Figure 13 shows a typical calculated Q values in an superplastic Al−Mg alloy. DUAN et al [138] calculated the *Q* values of Al−Mg−Mn−Zr alloys with Sc and Er addition as 84.8 and 87.2 kJ/mol, respectively, and proposed that GBS is the dominant superplastic deformation mechanism of the tested alloys. Through the study of AA6013 alloy, GHAYOUMABADI et al [12] found that with the addition of Y, Sc, and Zr, the superplasticity was enhanced, and the *Q* value of the alloys decreased from 154 to 95 kJ/mol, indicating that the deformation mechanism of the

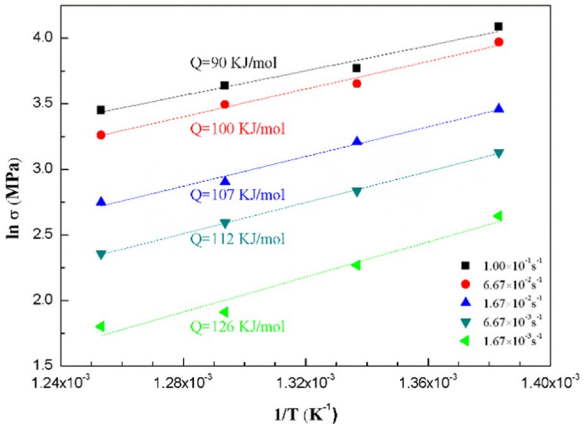

Fig. 13 Average Q value under different strain rates in superplastic Al−Mg−Sc−Zr alloy [140]

alloy gradually changed to GBS. ZHANG et al [13] noticed that the alloy with better superplasticity exhibited a calculated Q value closer to 84 kJ/mol, which proved that GBS played an important role in this alloy. More research on Q for superplastic Al alloys can also be found in works reported by BI et al [139], LI et al [140], and DUAN et al [14].

6 Quantitative research of superplastic deformation mechanism based on FIB-assisted surface study

6.1 Occurrence and development of surface study on superplastic deformation mechanism

The surface study is to investigate the evolution process of materials by recording their surface information before and after deformation. Surface study in bulk samples during superplastic deformation provides direct evidence of GBS, IDS, and DC, and it is one of the most effective methods to quantitatively study the superplastic deformation mechanism. There have been continuous studies trying to reveal the superplastic deformation mechanism by observing the surface structure characteristics during superplastic deformation and many theoretical deformation models have been proposed. The earliest surface research in superplasticity began in 1975 when HOTZ et al [141] made scratches on the polished sample surface by using diamond grinding paste, and then the scratches at the grain boundaries were found dislocated after deformation, thereby intuitively revealing the phenomenon of GBS during superplastic deformation. VALIEV and LANGDON [142] took the original features inside the grains as reference points and recorded their changes in the process of superplastic deformation, which proves the occurrence of IDS inside the grains. However, the above studies were conducted in random, and it is difficult to obtain reliable and repeatable surface studies with these methods.

With the development of FIB technology [143], researchers found that FIB could be used to mill high-resolution grids or lines on the alloy surface, and the superplastic deformation mechanism could be quantitatively analyzed by comparing the characterizations of these grids or lines before and after superplastic deformation [1]. RUST and TODD [144] carried out an FIB-aid surface study on 5083 Al alloy in the superplastic deformation Zone II and found that there was almost no deformation in the grains at strain of 5%−150%, indicating that there was no intra-granular dislocation movement, and the main superplastic deformation mechanism was GBS accommodated by DC. When investigating the superplastic deformation of Al−Mg−Mn alloy by using a FIB-aid surface study, MASUDA et al [119] noticed that grain rotation is an important accommodation mechanism of GBS. ZOU et al [25] proposed a modified Ashby−Verrall superplastic deformation model accompanied by IDS based on the FIB-aid surface study. LI et al [102] conducted FIB-aid surface studies on an Al−Zn−Mg−Cu alloy in a vacuum environment. They pointed out that the striated zones are the intergranular oxides formed by grain splitting, and a GBS model was proposed based on their findings. The combination of FIB and in-situ/quasi-in-situ electron microscopy enables researchers to re-examine the superplastic deformation mechanism proposed earlier by providing direct experimental evidence.

The typical papers on superplastic deformation research using FIB-aid surface study are listed in Table 1. According to Table 1, FIB-assisted surface study was widely used by researchers from 2008 in various superplastic Al alloys, and the largest true strain conducted for FIB-aid surface study ranges from 0.3 to 2.18. The largest true strain was achieved by SHEN et al [21], where the high-strain-rate superplastic deformation mechanism of an Al−Cu−Li alloy was quantitatively studied by three stages of quasi-in-situ SEM and FIB-assisted surface study in the true strain range of 0−2.8.

Table 1 Typical publications on superplastic deformation research by using FIB-aid surface study

Number	First author	Alloy	Largest true strain of surface study	Dominant superplastic deformation mechanism	Journal	Year
1	SHEN Zhi-xin [21]	Al−Cu−Li	2.18	GBS	J Mater Res Technol	2024
2	ZOU Guo-tong [25]	Al−Cu−Li	1.61	IDS at primary stage, GBS at second stage	Mater Sci Eng A	2023
3	LI Jun [145]	Al−Cu−Li	1.02	IDS	Mater Lett	2023
4	LI Guan-yu [102]	Al−Zn−Mg−Cu	1.1	GBS	Mater Sci Eng A	2022
5	LIU Xiao-dong [103]	Al−Cu−Li	0.71	DC	Mater Sci Eng A	2022
6	MIKHAYLOVSKAYA A V [19]	Al−Mg	1.0	DC	J Alloy Compd	2022
7	LIU Xiao-dong [23]	Al−Mg−Li	1.01	GBS	Mater Lett	2021
8	LIU Xiao-dong [125]	Al−Mg−Li	0.74	IDS at primary stage, GBS at second stage	Mater Sci Eng A	2021
9	MIKHAYLOVSKAYA A V [146]	Al−Zn−Mg−Cu	1.36	GBS and IDS	Mater Lett	2020
10	YAKOVTSEVA O A [147]	Al−Zn−Mg−Cu, Al−Mg−Mn	0.7	GBS	Mater Lett	2020
11	YAKOVTSEVA O A [148]	Al−Zn−Mg−Cu	1.0	GBS and DC	Mater Sci Eng A	2020
12	MIKHAYLOVSKAYA A V [149]	Al−Zn−Mg−Cu	1.59	DC at primary stage, GBS at steady stage	Mater Sci Eng A	2018
13	MASUDA H [119]	Al−Mg−Mn	0.25	GBS	Scripta Mater	2018
14	MIKHAYLOVSKAYA A V [101]	Al−Mg	0.4	DC	Mater Sci Eng A	2015
15	RUST M A [150]	Al−Mg−Mn	0.69	DC	Acta Mater	2011
16	SOTOUDEH K [100]	Al−Cu−Zr, Al−Mg−Mn	0.3	DC in Al−Mg−Mn	Acta Mater	2010
17	RUST M A [144]	Al−Mg−Mn	1.0	DC	Material Wissenschaft und Werkstofftechnik	2008

Based on the above cases, GBS, DC, and IDS have all been found to play a dominant role in various superplastic Al alloys, at least at a certain deformation stage. The superplastic deformation mechanism of Al alloy is related to the alloy composition, deformation parameter, grain structure, etc. Based on the summary in Table 1, by using FIB-aid surface study, it was found that the superplastic deformation of Al−Mg alloys is mainly controlled by DC, and that of Al−Zn alloy is mainly GBS. For those Al alloys with initial banded grain structure, GBS is difficult to occur at the initial stage of deformation due to the banded grain boundaries; therefore, IDS is the dominant deformation mechanism. When the dynamic recrystallization is accomplished, the main deformation mechanism will transform from the IDS into GBS due to the increase of HAGBs fraction.

6.2 Main methodology of FIB-aid surface study

The typical FIB milled grids are shown in Fig. 14. The coarse grids are used to observe the offsets of grain boundaries, the fine grids are used to observe the intragranular deformation after deformation, and the size of milled grinds depends on the grain size. Normally, samples should be polished mechanically before FIB milling. After being milled, in-situ/quasi-in-situ superplastic deformation can be carried out on the test samples, and vacuum protection or anti-oxidant protection is necessary to prevent oxidation from affecting the surface morphology. To capture usable surface information, the strain of each step of deformation

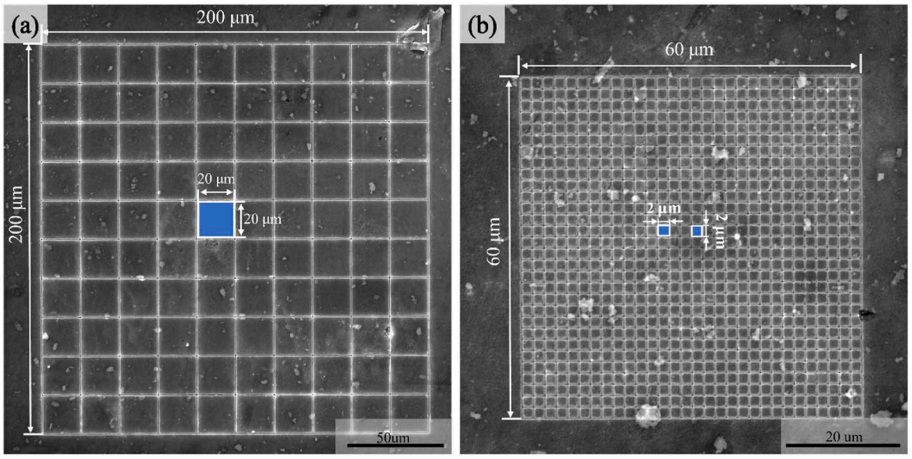

Fig. 14 Typical FIB-etched grids for surface study [25]: (a) Coarse grids; (b) Fine grids

should be strictly controlled, and a true strain of 0.2−0.4 is suitable for most superplastic Al alloys. By comparing the SEM images of the surface before and after each step of deformation, the features of every superplastic deformation mechanism can be analyzed and their contribution to total strain can be calculated quantitatively.

The contribution of GBS to the total superplastic strain can be calculated by using the following formula [151]:

$$\varepsilon_{\mathrm{GBS}}=\sum\left(u_i \tan\theta_i\right)/l_0 \tag{5}$$

$$\varepsilon_{\mathrm{tot}}=\left(l_0-l\right)/l_0 \tag{6}$$

$$\gamma_{\mathrm{GBS}}=\varepsilon_{\mathrm{GBS}}/\varepsilon_{\mathrm{tot}}=\sum\left(u_i \tan\theta_i\right)/\left(l_0-l\right) \tag{7}$$

where $\varepsilon_{\mathrm{GBS}}$ is the strain caused by GBS, u_i is the offset component along the stretched axis at the ith grain boundary, θ_i is the angle between the ith grain boundary and the stretched axis, l_0 is the length of the grid line perpendicular to the stretched axis before the tensile test, $\varepsilon_{\mathrm{tot}}$ is the total strain transverse to the tensile axis, l is the length of the fine grid line perpendicular to the stretched axis after the tensile test, and γ_{GBS} is the contribution of GBS to the total strain.

The contribution of IDS is determined by calculating the spacing changes before and after every stage of deformation of fine grid lines inside the grains [142], and the following equation can be used:

$$\varepsilon_{\mathrm{IDS}}=\sum\left(a-a_0\right)/a_0 \tag{8}$$

$$\gamma_{\mathrm{IDS}}=\varepsilon_{\mathrm{IDS}}/\varepsilon_{\mathrm{tot}} \tag{9}$$

where $\varepsilon_{\mathrm{IDS}}$ is the strain induced by GBS, a_0 is the length of the grid line inside a grain before deformation, a is the length of the same grid line after deformation, and the grid line length is measured along the tension direction, and γ_{IDS} is the contribution of IDS to the total strain.

The contribution of DC can be obtained by subtracting the contribution of GBS and IDS from 100% [13,125], or by calculating the proportion of the total length of striated zones to diffusion zones in the total strain in a certain region [136,149].

6.3 Typical research cases on superplastic deformation mechanism in Al alloys

Figure 15 shows the SEM images of the FIB-aid surface study conducted on AA3003 alloy (with initial banded grains, and no superplasticity) and AA5083 alloy (with initial equiaxed grains and superplastic true strain of more than 1.4) [100]. The offsets of coarse grid lines in both alloys can be observed, but the fine grid lines inside the grains of AA3003 exhibit greater deformation than those of AA5083. The extension zones are significant features in AA5083. By carrying out quantitative calculations of the intergranular and intragranular deformation, it was found that the values of intergranular deformation in the two alloys are similar, but the intragranular strain in AA3003 is twice that of AA5083. According to the FIB-aid surface study and quantitative analysis, the DC is considered responsible for the superplasticity of AA5083 due to its high solute content and self-diffusion.

By conducting a careful FIB-assisted surface study, ZOU et al [25] analyzed the superplastic deformation mechanisms of a banded-grained 2A97

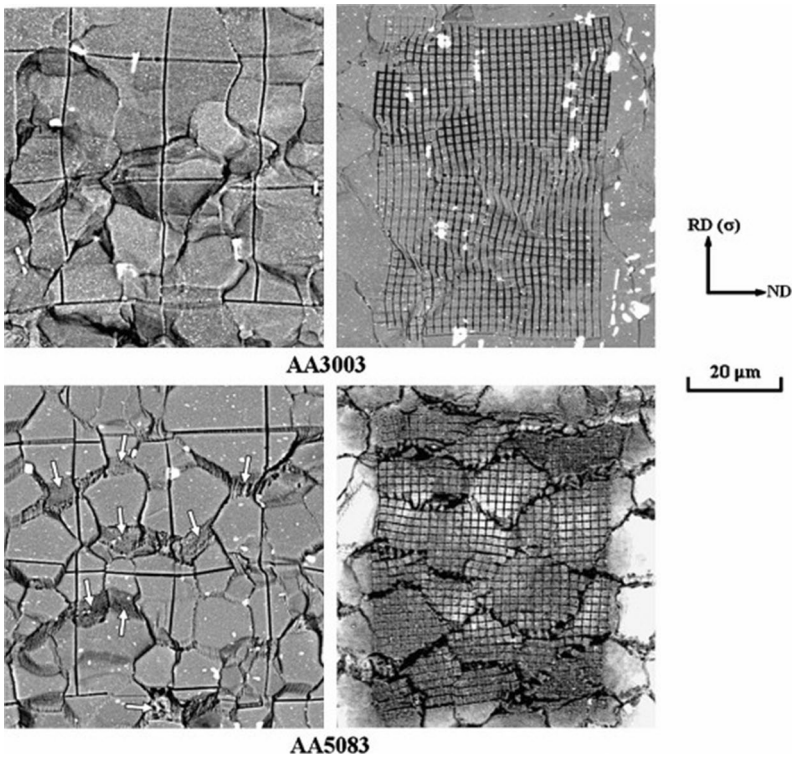

Fig. 15 SEM images of grids on polished surfaces of AA3003 and AA5083 deformed to average strain of 0.3 at 530 °C and 5×10^{-1} s^{-1} [100]

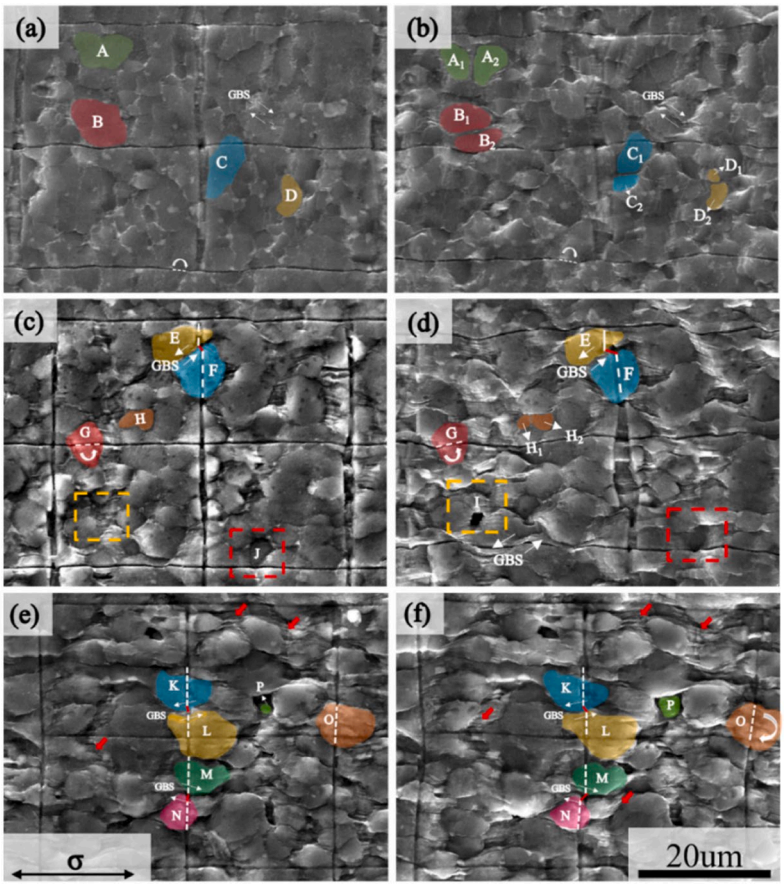

Fig. 16 SEM images showing evolution of coarse grids in 2A97 Al−Cu−Li alloy during quasi-in-situ superplastic deformation [25]

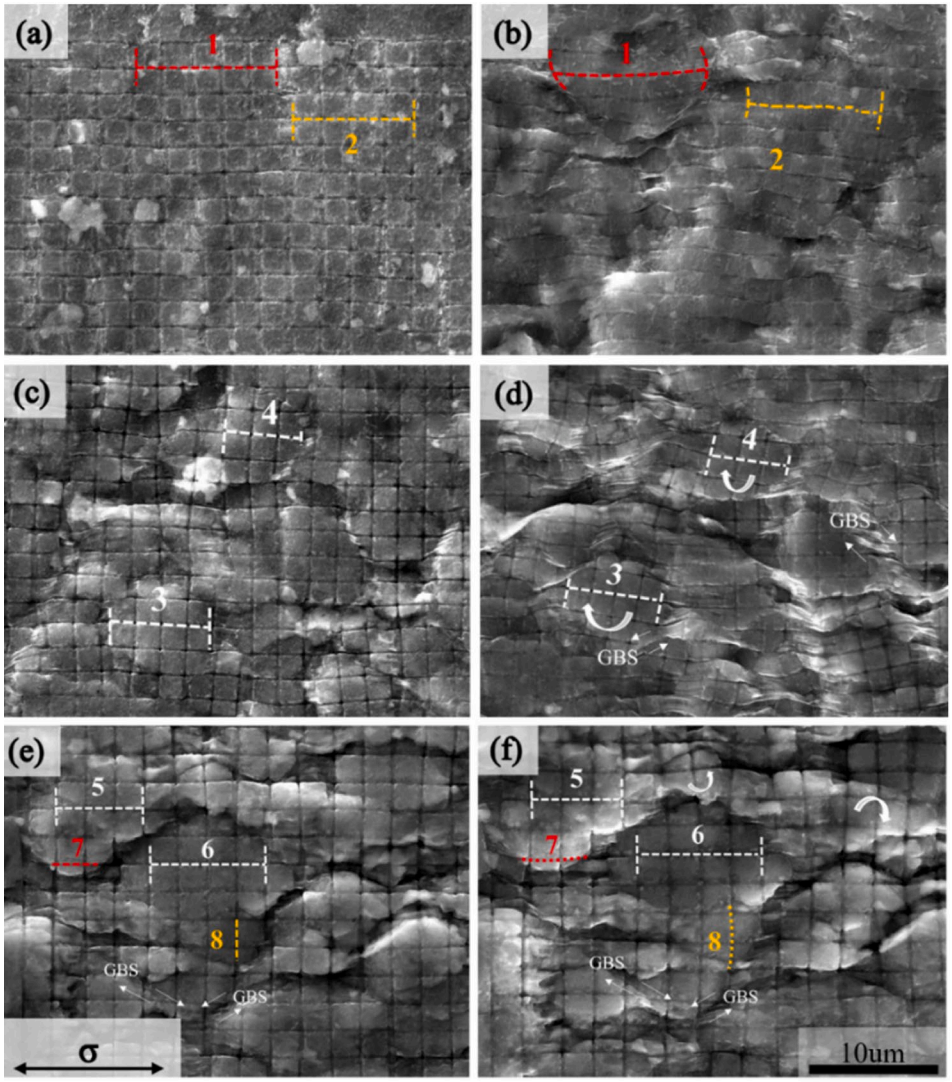

Fig. 17 SEM images showing evolution of fine grids in 2A97 Al−Cu−Li alloy during quasi-in-situ superplastic deformation [25]

Al−Cu−Li alloy under a large true strain range (0−1.61). As shown in Figs. 16 and 17, in the initial deformation stage, "grain splitting" phenomenon can be observed from Figs. 16(a, b), and the fine grid lines can be found elongated and bent from Figs. 17(a, b), which is evidence of intragranular deformation and dynamic recrystallization. When the deformation comes to the second stage, from Figs. 16(c−f), significant GBS, grain rotation, grain drowning, and grain floating can be observed. These evidences prove that the superplastic deformation mechanism of the studied alloy transforms from IDS to GBS with the increase of true strain, which is consistent with the quantitative calculation results (the maximum contribution of IDS is ~54.1% at the true strain of 0.74, and the contribution of GBS is more than 50% with the true strain larger than 1.1).

Figures 18 and 19 show SEM images of a fine-grained Al−Cu−Li superplastic alloy with the FIB-aid surface study [103]. By tracking the evolution of representative grains with the true strain of 0.13−0.71, obvious grain rotation (Grain A) and relative grain motion can be found. According to the surface images before and after deformation, the fine grids in grains have little change, which indicates insignificant intragranular deformation. Significant striated zones can be noticed among grains, which is the manifestation of DC. By calculating the contribution of different superplastic deformation mechanisms to the total strain, it is found that the contribution of GBS and IDS are not much, with the largest contribution of GBS of (33.1±4.6)%, and the largest contribution of

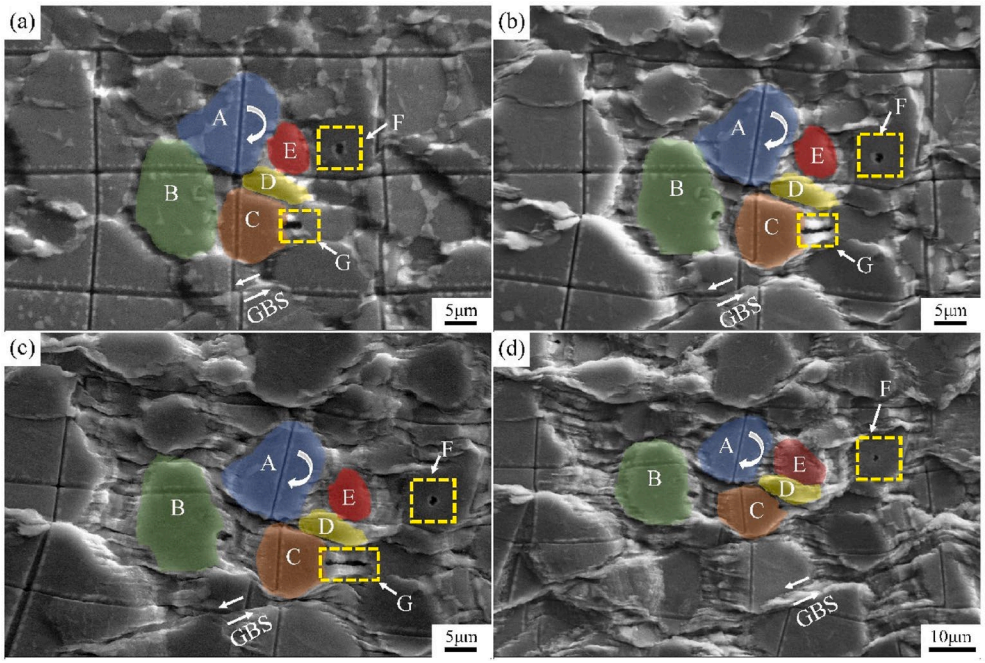

Fig. 18 Evolution of coarse grids in fine-grained superplastic Al−Cu−Li alloy with different true strains [103]: (a) 0.13; (b) 0.29; (c) 0.52; (d) 0.71

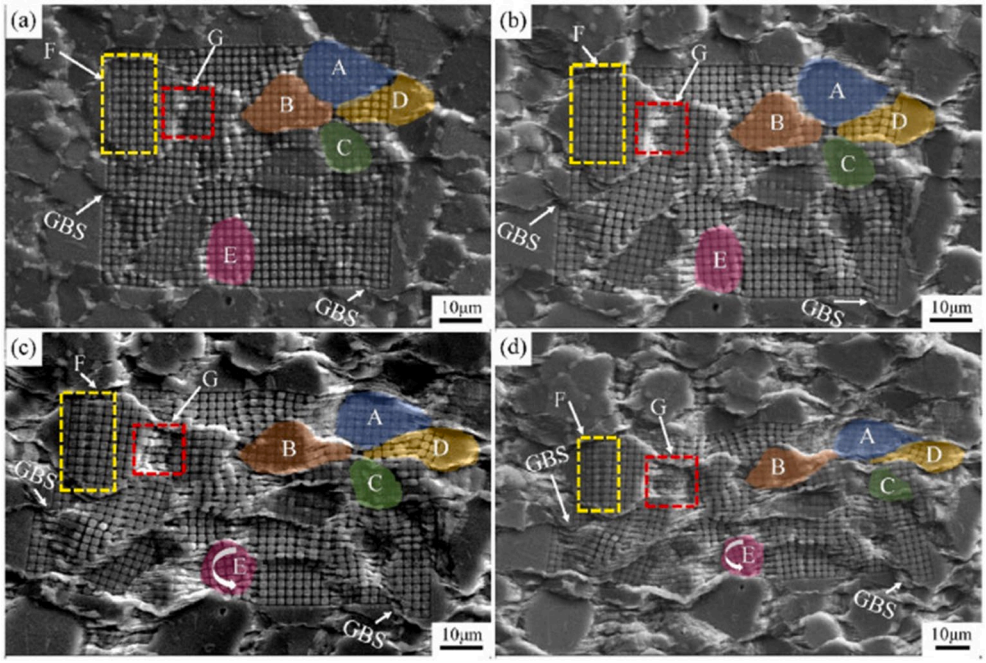

Fig. 19 Evolution of fine grids in fine-grained superplastic Al−Cu−Li alloy with different true strains [103]: (a) 0.13; (b) 0.29; (c) 0.52; (d) 0.71

IDS of (9.2±1.1)%. Therefore, the authors attributed the dominant superplastic deformation mechanism to DC. GBS and IDS played accommodating mechanisms.

MIKHAYLOVSKAYA et al [149] compared the superplastic deformation mechanisms of a fine grain AA7475 alloy at the primary stage (the true strain of 0−0.69) and steady stage (the true strain of 0.69−1.59) by using FIB-aid surface study. In the SEM images of coarse grid evolution shown in Fig. 20, grain neighbour switching and grain rotation can be noticed in various strain ranges, but these phenomena are more intensive at the steady stage. For the observation of fine grids, as shown in Fig. 21, it can be found that the grid lines maintain their initial configurations in the centre of the grains,

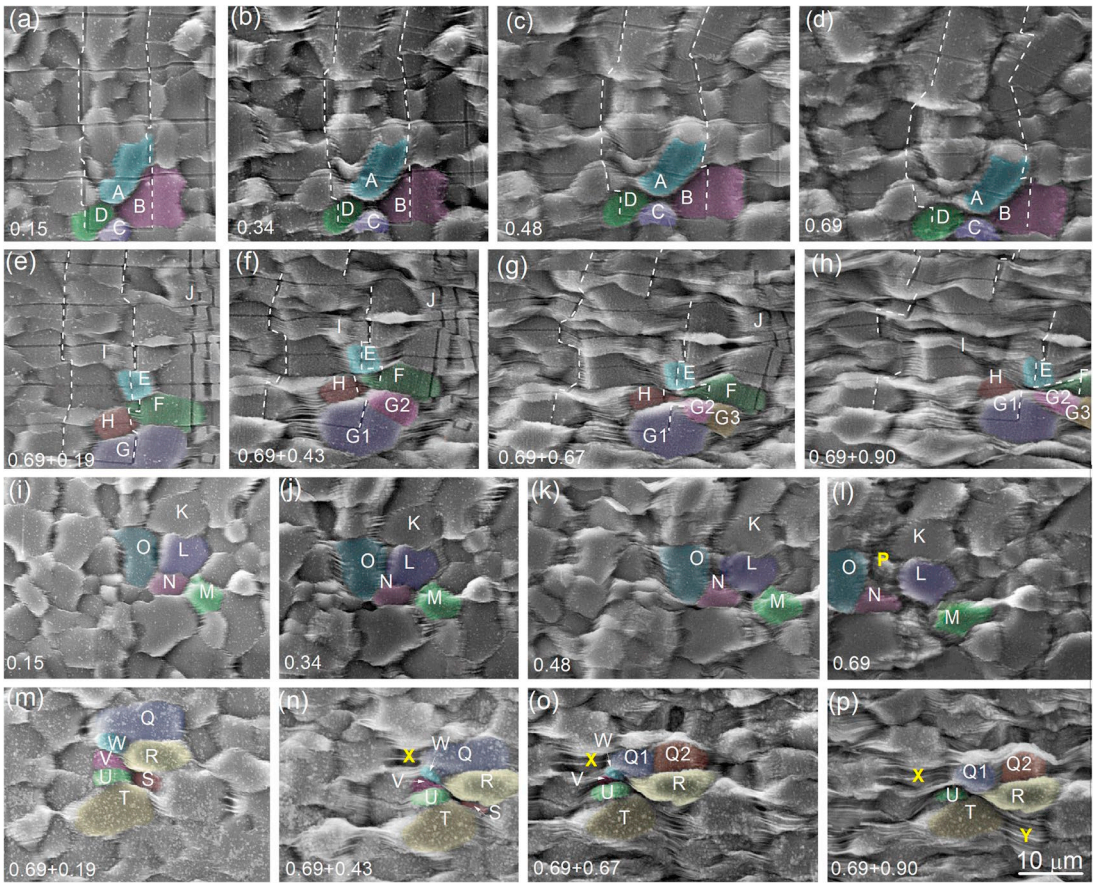

Fig. 20 Surface study of fine-grain AA7475 alloy during superplastic deformation [149]: (a−d, i−l) In primary stage; (e−h, m−p) In steady stage

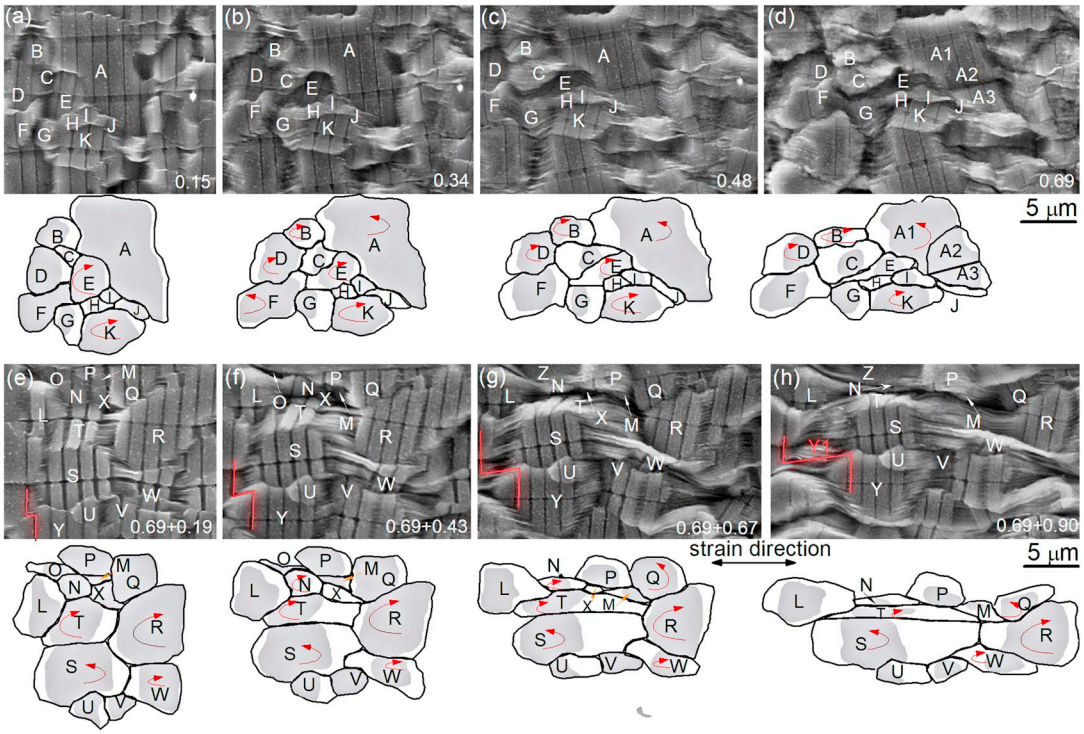

Fig. 21 Local area observation of fine-grain AA7475 alloy during superplastic deformation [149]: (a−d) In primary stage; (e−h) In steady stage

which indicates that IDS plays little role. The quantitative analysis shows that the GBS accounts for 30%−40% at the primary stage and increases to 50%−60% at the steady stage of deformation, and DC plays an important role during the whole deformation range.

7 Summary and conclusions

(1) Superplastic Al alloys have a profound research foundation and are widely used in aerospace, automobile, and rail transit, etc. The development tendency of superplastic Al alloys is to obtain superplasticity at low temperature and/or high strain rate, and the superplastic forming (SPF) of Al alloys is developing into the direction of high quality and low cost.

(2) Fine, equiaxed, and stable grain structures are very important for superplastic Al alloys, and Sc and Zr elements are commonly used in Al alloys to refine and stabilize grains. For superplastic Al alloys with an initial banded (unrecrystallized) structure, obtaining fine and equiaxed grains via dynamic recrystallization during deformation is the guarantee of superplastic elongation. Texture evolution and cavitation are affected by the superplastic deformation mechanism. The texture, coarsening of secondary phases, and cavities have an adverse influence on the Al alloys after superplastic deformation.

(3) Deformation behaviour parameters such as strain rate sensitivity (m) and activation energy (Q) can reflect the superplastic deformation mechanisms of Al alloy. Grain boundary sliding (GBS) plays an important role in superplastic Al alloys. The m value corresponding to GBS is ~0.5, and the Q value corresponding to GBS is ~84 kJ/mol.

(4) FIB-aid surface study is one of the widely used methods for investigating the superplastic deformation mechanism of aluminum alloys. The contribution of different deformation mechanisms such as grain boundary sliding (GBS), intragranular dislocation slip (IDS), and diffusion creep (DC) can be calculated quantitatively. Some new insights and new models of deformation mechanisms for superplastic Al alloys are proposed based on the FIB-aid surface study, such as a modified Ashby−Verrall model accompanied by IDS, tracking the evolution of dominant deformation mechanisms in the whole superplastic deformation stage.

CRediT authorship contribution statement

Guo-tong ZOU: Methodology; Investigation, Writing − Original draft; **Shi-jie CHEN:** Methodology, Investigation; **Ya-qi XU:** Investigation; **Bao-kun SHEN:** Investigation; **Yu-jia ZHANG:** Investigation; **Ling-ying YE**: Supervision, Writing − Review & editing.

Declaration of competing interest

The authors declare that they have no known competing financial interests or personal relationships that could have appeared to influence the work reported in this paper.

References

[1] LANGDON T G. Seventy-five years of superplasticity: Historic developments and new opportunities [J]. Journal of Materials Science, 2009, 44: 5998−6010.

[2] BHATTA L, PESIN A, ZHILYAEV A P, TANDON P, KONG C, YU Hai-liang. Recent development of superplasticity in aluminum alloys: A review [J]. Metals, 2020, 10: 77.

[3] WANG Si-qing, ZHA Min, JIA Hai-long, YANG Ya-jie, WANG Da-wei, WANG Cheng, GAO Yi-peng, WANG Hui-Yuan. A review of superplastic magnesium alloys: Focusing on alloying strategy, grain structure control and deformation mechanisms [J]. Journal of Materials Science & Technology, 2025, 211: 303−319.

[4] BARNES A J. Superplastic forming 40 years and still growing [J]. Journal of Materials Engineering and Performance, 2013, 22: 2935−2949.

[5] WANG Xiao-guo, LI Qiu-shu, WU Rui-rui, ZHANG Xiao-yuan, MA Li-yun. A review on superplastic formation behavior of Al alloys [J]. Advances in Materials Science and Engineering, 2018, 2018: 1−17.

[6] MASUDA H, SATO E. Diffusional and dislocation accommodation mechanisms in superplastic materials [J]. Acta Materialia, 2020, 197: 235−252.

[7] XING H L, WANG C W, ZHANG K F, WANG Z R. Recent development in the mechanics of superplasticity and its applications [J]. Journal of Materials Processing Technology, 2004, 151: 196−202.

[8] BATE P S, RIDLEY N, ZHANG B. Mechanical behaviour and microstructural evolution in superplastic Al−Li−Mg−Cu−Zr AA8090 [J]. Acta Materialia, 2007, 55: 4995−5006.

[9] WANG Zeng-yu, YANG Zhi-ting, JIANG Sen-bao, WANG Yus-heng, CHEN Yao, LI Xi-feng, WANG Qu-dong. Effect of temperature on superplastic deformation behavior of 2198 Al−Cu−Li alloy [J]. Materials Science and Engineering A, 2024, 891: 145988.

[10] ZOU Guo-tong, XU Ya-qi, LI Jun, SHEN Zhi-xin, YE Ling-ying. Effect of superplastic deformation on microstructures, texture, and mechanical properties of 2A97 Al−Cu−Li alloy [J]. Materials Science and Engineering A, 2024, 891: 145972.

[11] CAO Fu-rong, TENG Xiao-ming, SU Rui-kang, LIANG Jin-rui, LIU Ren-jie, KONG Shu-ting, GUO Nan-pan. Room temperature strengthening mechanisms, high temperature

deformation behavior and constitutive modeling in an Al−3.25Mg−0.37Zr−0.28Mn−0.19Y alloy [J]. Journal of Materials Research and Technology, 2022, 18: 962−977.

[12] GHAYOUMABADI M E, MOCHUGOVSKIY A G, TABACHKOVA N Y, MIKHAYLOVSKAYA A V. The influence of minor additions of Y, Sc, and Zr on the microstructural evolution, superplastic behavior, and mechanical properties of AA6013 alloy [J]. Journal of Alloys and Compounds, 2022, 900: 163477.

[13] ZHANG Hong-min, JIANG Peng, PAN Hai-jun, PENG Jian, WANG Zhi-zhi, YAN Ke-tao, ZHA Min. Dynamic recrystallization-dependent high-temperature tensile properties and deformation mechanisms in Al−Mg−Sc−Zr alloys [J]. Materials Science and Engineering A, 2023, 880: 145304.

[14] DUAN Y L, TANG L, DENG Y, CAO X W, XU G F, YIN Z M. Superplastic behavior and microstructure evolution of a new Al−Mg−Sc−Zr alloy subjected to a simple thermomechanical processing [J]. Materials Science and Engineering A, 2016, 669: 205−217.

[15] XIANG H, PAN Q L, YU X H, HUANG X, SUN X, WANG X D, LI M J, YIN Z M. Superplasticity behaviors of Al−Zn−Mg−Zr cold-rolled alloy sheet with minor Sc addition [J]. Materials Science and Engineering A, 2016, 676: 128−137.

[16] KOTOV A D, MIKHAYLOVSKAYA A V, KISHCHIK M S, TSARKOV A A, AKSENOV S A, PORTNOY V K. Superplasticity of high-strength Al-based alloys produced by thermomechanical treatment [J]. Journal of Alloys and Compounds, 2016, 688: 336−344.

[17] ARUN B K, SUBRAMANYA S V, ATHREYA C N, PADMANABHAN K A. Experimental verification of grain boundary-sliding controlled steady state superplastic flow in both continually and statically recrystallizing Al alloys [J]. Materials Science and Engineering A, 2016, 657: 185−196.

[18] LI Guang-yu, DING Hua, WANG Jian. A new set of physically-based unified viscoplastic constitutive equations for superplastic deformation of Al−Zn−Mg−Cu alloy [J]. Mechanics Research Communications, 2022, 123: 103904.

[19] MIKHAYLOVSKAYA A V, YAKOVTSEVA O A, MOCHUGOVSKIY A G, CIFRE J, GOLOVIN I S. Influence of minor Zn additions on grain boundary anelasticity, grain boundary sliding, and superplasticity of Al−Mg-based alloys [J]. Journal of Alloys and Compounds, 2022, 926: 166785.

[20] MIKHAYLOVSKAYA A V, YAKOVTSEVA O A, IRZHAK A V. The role of grain boundary sliding and intragranular deformation mechanisms for a steady stage of superplastic flow for Al−Mg-based alloys [J]. Materials Science and Engineering A, 2022, 833: 142524.

[21] SHEN Zhi-xin, ZOU Guo-tong, DONG Yu, ZHANG Yu-jia, YE Ling-ying. In-situ surface study on the mechanism of high-strain-rate superplasticity in an Al−Cu−Li alloy [J]. Journal of Materials Research and Technology, 2024, 28: 2815−2818.

[22] MIKHAYLOVSKAYA A V, GHAYOUMABADI M E, MOCHUGOVSKIY A G. Superplasticity and mechanical properties of Al−Mg−Si alloy doped with eutectic-forming Ni and Fe, and dispersoid-forming Sc and Zr elements [J]. Materials Science and Engineering A, 2021, 817: 141319.

[23] LIU Xiao-dong, YE Ling-ying, TANG Jian-guo, DONG Yu, KE Bin. Superplastic deformation mechanism of an Al−Mg−Li alloy by high resolution surface studies [J]. Materials Letters, 2021, 301: 130251.

[24] MOCHUGOVSKIY A G, MIKHAYLOVSKAYA A V, ZADOROGNYY M Y, GOLOVIN I S. Effect of heat treatment on the grain size control, superplasticity, internal friction, and mechanical properties of zirconium-bearing aluminum-based alloy [J]. Journal of Alloys and Compounds, 2021, 856: 157455.

[25] ZOU Guo-tong, YE Ling-ying, LI Jun, SHEN Zhi-xin. Microstructure evolution and deformation mechanisms of a banded-grained 2A97 Al−Cu−Li alloy during superplastic deformation [J]. Materials Science and Engineering A, 2023, 876: 145178.

[26] SHEN Zhi-xin, YE Ling-ying, LIU Xiao-dong, DONG Yu. Achieving high strain rate superplasticity in an Al−Cu−Li alloy processed by thermo-mechanical processing [J]. Materials Letters, 2023, 340: 134142.

[27] BOCHVAR A A, SVIDERSKAYA Z A. Superplasticity in zinc−aluminum alloys [J]. Bull Acad Sci URSS, Classe Sci Tech, 1945, 9: 821−824.

[28] MACHADO D C, FLAUSINO P C A, HUANG Yi, CETLIN P R, LANGDON T G, PEREIRA P H R. Influence of processing temperature on microhardness evolution, microstructure and superplastic behaviour in an Al−Mg alloy processed by high-pressure torsion [J]. Journal of Materials Research and Technology, 2023, 24: 2850−2867.

[29] SONG Zi-zheng, NIU Ran-ming, CUI Xiang-yuan, BOBRUK E V, MURASHKIN M Y, ENIKEEV N A, GU Ji, SONG Min, BHATIA V, RINGER S P, VALIEV R Z, LIAO Xiao-zhou. Mechanism of room-temperature superplasticity in ultrafine-grained Al−Zn alloys [J]. Acta Materialia, 2023, 246: 118671.

[30] BOBRUK E V, SAFARGALINA Z A, GOLUBEV O V, BAYKOV D, KAZYKHANOV V U. The effect of ultrafine-grained states on superplastic behavior of Al−Mg−Si alloy [J]. Materials Letters, 2019, 255: 126503.

[31] BOBRUK E V, SAUVAGE X, ENIKEEV N A, VALIEV R Z. Influence of fine scale features on room temperature superplastic behaviour of an ultrafine-grained Al−30Zn alloy [J]. Materials Letters, 2019, 254: 329−331.

[32] ALHAMIDI A, HORITA Z. Grain refinement and high strain rate superplasticity in alumunium 2024 alloy processed by high-pressure torsion [J]. Materials Science and Engineering A, 2015, 622: 139−145.

[33] KRASILNIKOV N A, SHARAFUTDINIV A. High strength and ductility of nanostructured Al-based alloy, prepared by high-pressure technique [J]. Materials Science and Engineering A, 2007, 463: 74−77.

[34] GARCIA-INFANTA J M, ZHILYAEV A P, SHARAFUTDINOV A, RUANO O A, CARRENO F. An evidence of high strain rate superplasticity at intermediate homologous temperatures in an Al−Zn−Mg−Cu alloy processed by high-pressure torsion [J]. Journal of Alloys and Compounds, 2009, 473: 163−166.

[35] XU Cheng, DOBATKIN S V, HORITA Z, LANGDON T G. Superplastic flow in a nanostructured aluminum alloy

produced using high-pressure torsion [J]. Materials Science and Engineering A, 2009, 500: 170−175.

[36] KAWASAKI M, FOISSEY J, LANGDON T G. Development of hardness homogeneity and superplastic behavior in an aluminum−copper eutectic alloy processed by high-pressure torsion [J]. Materials Science and Engineering A, 2013, 561: 118−125.

[37] LU Piao-qi, HUANG Hong-feng, REN Qian-qian, YANG Jia-nan, WEI Li-li, LIU Shu-hui, XU Xu-da, XIE Hu. Effect of initial grain structure on the microstructure evolution and superplastic behavior of Al−Mg−Sc−Zr alloy [J]. Materials Characterization, 2024, 210: 113792.

[38] ALBERTO O C, MARTA A L, PALOMA H M, CARMEN M C, OSCAR A R, FERNANDO C. Grain size versus microstructural stability in the high strain rate superplastic response of a severely friction stir processed Al−Zn−Mg−Cu alloy [J]. Materials Science and Engineering A, 2017, 680: 329−337.

[39] PATEL V V, BADHEKA V, KUMAR A. Effect of polygonal pin profiles on friction stir processed superplasticity of AA7075 alloy [J]. Journal of Materials Processing Technology, 2017, 240: 68−76.

[40] ALBERTO O C, MARTA A L, DAVID V, PILAR R, OSCAR A R, FERNANDO C. Evaluation of the mechanical anisotropy and the deformation mechanism in a multi-pass friction stir processed Al−Zn−Mg−Cu alloy [J]. Materials & Design, 2017, 125: 116−125.

[41] MA Z Y, MISHRA R S, MAHONEY M W, GRIMES R. High strain rate superplasticity in friction stir processed Al−Mg−Zr alloy [J]. Materials Science and Engineering A, 2003, 351: 148−153.

[42] CHARIT I, MISHRA R S. High strain rate superplasticity in a commercial 2024 Al alloy via friction stir processing [J]. Materials Science and Engineering A, 2003, 359: 290−296.

[43] CHARIT I, MISHRA R S. Low temperature superplasticity in a friction-stir-processed ultrafine grained Al−Zn−Mg−Sc alloy [J]. Acta Materialia, 2005, 53: 4211−4223.

[44] DUTTA A, CHARIT I, JOHANNES L B, MISHRA R S. Deep cup forming by superplastic punch stretching of friction stir processed 7075 Al alloy [J]. Materials Science and Engineering A, 2005, 395: 173−179.

[45] MA Z Y, MISHRA R S. Development of ultrafine-grained microstructure and low temperature ($0.48T_m$) superplasticity in friction stir processed Al−Mg−Zr [J]. Scripta Materialia, 2005, 53: 75−80.

[46] WANG Y, MISHRA R S. Finite element simulation of selective superplastic forming of friction stir processed 7075 Al alloy [J]. Materials Science and Engineering A, 2007, 463: 245−248.

[47] LIU F C, MA Z Y, CHEN L Q. Low-temperature superplasticity of Al−Mg−Sc alloy produced by friction stir processing [J]. Scripta Materialia, 2009, 60: 968−971.

[48] GARCIA-BERNAL M A, MISHRA R S, VERMA R, HERNANDEZ-SILVA D. High strain rate superplasticity in continuous cast Al−Mg alloys prepared via friction stir processing [J]. Scripta Materialia, 2009, 60: 850−853.

[49] WANG K, LIU F C, MA Z Y, ZHANG F C. Realization of exceptionally high elongation at high strain rate in a friction stir processed Al−Zn−Mg−Cu alloy with the presence of liquid phase [J]. Scripta Materialia, 2011, 64: 572−575.

[50] OROZCO-CABALLERO A, CEPEDA-JIMÉNEZ C M, HIDALGO-MANRIQUE P, REY P, GESTO D, VERDERA D, RUANO O A, CARREÑO F. Lowering the temperature for high strain rate superplasticity in an Al−Mg−Zn−Cu alloy via cooled friction stir processing [J]. Materials Chemistry and Physics, 2013, 142: 182−185.

[51] GARCÍA-BERNAL M A, MISHRA R S, VERMA R, HERN7UNDEZ-SILVA D. Inhibition of abnormal grain growth during hot deformation behavior of friction stir processed 5083 Al alloys [J]. Materials Science and Engineering A, 2015, 636: 326−330.

[52] SUN Y B, CHEN X P, XIE J, WANG C, AN Y F, LIU Q. High strain rate superplasticity and secondary strain hardening of Al−Mg−Sc−Zr alloy produced by friction stir processing [J]. Materials Today Communications, 2022, 33: 104217.

[53] LIU F C, MA Z Y. Achieving exceptionally high superplasticity at high strain rates in a micrograined Al−Mg−Sc alloy produced by friction stir processing [J]. Scripta Materialia, 2008, 59: 882−885.

[54] LIU F C, MA Z Y. Low-temperature superplasticity of friction stir processed Al−Zn−Mg−Cu alloy [J]. Scripta Materialia, 2008, 58: 667−670.

[55] MA Z Y, LIU F C, MISHRA R S. Superplastic deformation mechanism of an ultrafine-grained aluminum alloy produced by friction stir processing [J]. Acta Materialia, 2010, 58: 4693−4704.

[56] LIU F C, XIAO B L, WANG K, MA Z Y. Investigation of superplasticity in friction stir processed 2219Al alloy [J]. Materials Science and Engineering A, 2010, 527: 4191−4196.

[57] LIU F C, MA Z Y. Contribution of grain boundary sliding in low-temperature superplasticity of ultrafine-grained aluminum alloys [J]. Scripta Materialia, 2010, 62: 125−128.

[58] LIU F C, MA Z Y, ZHANG F C. High strain rate superplasticity in a micro-grained Al−Mg−Sc alloy with predominant high angle grain boundaries [J]. Journal of Materials Science & Technology, 2012, 28: 1025−1030.

[59] LIU F C, XUE P, MA Z Y. Microstructural evolution in recrystallized and unrecrystallized A−Mg−Sc alloys during superplastic deformation [J]. Materials Science and Engineering A, 2012, 547: 55−63.

[60] SMOLEJ A, KLOBČAR D, SKAZA B, NAGODE A, SLAČEK E, DRAGOJEVIĆ V, SMOLEJ S. Superplasticity of the rolled and friction stir processed Al−4.5Mg−0.35Sc−0.15Zr alloy [J]. Materials Science and Engineering A, 2014, 590: 239−245.

[61] GARCÍA-BERNAL M A, MISHRA R S, VERMA R, HERNÁNDEZ-SILVA D. Influence of friction stir processing tool design on microstructure and superplastic behavior of Al−Mg alloys [J]. Materials Science and Engineering A, 2016, 670: 9−16.

[62] GAN Wen-ying, ZHOU Zheng, ZHANG Hang, PENG Tao. Evolution of microstructure and hardness of aluminum after friction stir processing [J]. Transactions of Nonferrous Metals Society of China, 2014, 24: 975−981.

[63] LIU Zhi-hao, HAN Peng, WANG Wen, GUAN Xiao-hu, WANG Zhi, FANG Yuan, QIAO Ke, YE Dong-ming, CAI

Jun, XIE Ying-chun, WANG Kuai-she. Microstructure, mechanical properties, and corrosion behavior of 6061Al alloy prepared by cold spray-friction stir processing composite additive manufacturing [J]. Transactions of Nonferrous Metals Society of China, 2023, 33: 3250−3265.

[64] CHUVIL'DEEV V N, GRYAZNOV M Y, SHOTIN S V, NOKHRIN A V, LIKHNITSKII C V, NAGICHEVA G S, CHEGUROV M K, KOPYLOV V I, BOBROV A A, SHADRINA I S. Effect of Sc/Zr ratio on superplastic behavior of ultrafine-grained Al−6%Mg alloys [J]. Materials Science and Engineering A, 2024, 898: 146409.

[65] MYSHLYAEV M, MIRONOV S, KORZNIKOVA G, KONKOVA T, KORZNIKOVA E, ALETDINOV A, KHALIKOVA G, RAAB G, SEMIATIN S L. EBSD study of superplasticity: New insight into a well-known phenomenon [J]. Journal of Alloys and Compounds, 2022, 898: 162949.

[66] MYSHLYAEV M, KORZNIKOVA G, KONKOVA T, KORZNIKOVA E, ALETDINOV A, KHALIKOVA G, RAAB G, MIRONOV S. Microstructural evolution during superplastic deformation of Al−Mg−Li alloy: Dynamic recrystallization or grain-boundary sliding? [J]. Journal of Alloys and Compounds, 2023, 936: 168302.

[67] SITDIKOV O, AVTOKRATOVA E, LATYPOVA O, MARKUSHEV M. Structure, strength and superplasticity of ultrafine-grained 1570C aluminum alloy subjected to different thermomechanical processing routes based on severe plastic deformation [J]. Transactions of Nonferrous Metals Society of China, 2021, 31: 887−900.

[68] CHUVIL'DEEV V N, GRYAZNOV M Y, SHOTIN S V, KOPYLOV V I, NOKHRIN A V, LIKHNITSKII C V, MURASHOV A A, BOBROV A A, TABACHKOVA N Y, PIROZHNIKOVA O E. Investigation of superplasticity and dynamic grain growth in ultrafine-grained Al−0.5%Mg−Sc alloys [J]. Journal of Alloys and Compounds, 2021, 877: 160099.

[69] BALASUBRAMANIAN N, LANGDON T G. An analysis of superplastic flow after processing by ECAP [J]. Materials Science and Engineering A, 2005, 410/411: 476−479.

[70] KAWASAKI M, XU Cheng, LANGDON T G. An investigation of cavity growth in a superplastic aluminum alloy processed by ECAP [J]. Acta Materialia, 2005, 53: 5353−5364.

[71] KYUNG-TAE P, HANG-JAE L, CHONG S L, SHIN H S. Effect of post-rolling after ECAP on deformation behavior of ECAPed commercial Al−Mg alloy at 723 K [J]. Materials Science and Engineering A, 2005, 393: 118−124.

[72] XU Cheng, LANGDON T G. Creep and superplasticity in a spray-cast aluminum alloy processed by ECA pressing [J]. Materials Science and Engineering A, 2005, 410/411: 398−401.

[73] XU Cheng, FURUKAWA M, HORITA Z, LANGDON T G. Influence of ECAP on precipitate distributions in a spray-cast aluminum alloy [J]. Acta Materialia, 2005, 53: 749−758.

[74] MÁLEK P, TURBA K, CIESLAR M, DRBOHLAV I, KRUML T. Structure development during superplastic deformation of an Al−Mg−Sc−Zr alloy [J]. Materials Science and Engineering A, 2007, 462: 95−99.

[75] YOUNG G K, DONG H S, KYUNG-TAE P, CHONG S L. Superplastic deformation behavior of ultra-fine-grained 5083 Al alloy using load-relaxation tests [J]. Materials Science and Engineering A, 2007, 449/450/451: 756−760.

[76] TURBA K, MÁLEK P, CIESLAR M. Superplasticity in an Al−Mg−Zr−Sc alloy produced by equal-channel angular pressing [J]. Materials Science and Engineering A, 2007, 462: 91−94.

[77] CEPEDA-JIMÉNEZ C M, GARCÍA-INFANTA J M, RUANO O A, CARREÑO F. High strain rate superplasticity at intermediate temperatures of the Al 7075 alloy severely processed by equal channel angular pressing [J]. Journal of Alloys and Compounds, 2011, 509: 9589−9597.

[78] CEPEDA-JIMÉNEZ C M, GARCÍA-INFANTA J M, RUANO O A, CARREÑO F. Achieving microstructures prone to superplastic deformation in an Al−Zn−Mg−Cu alloy by equal channel angular pressing [J]. Journal of Alloys and Compounds, 2013, 546: 253−259.

[79] ZHA Min, ZHANG Hong-min, JIA Hai-long, GAO Yi-peng, JIN Shen-bao, SHA Gang, BJØRGE R, MATHIESEN R H, ROVEN H J, WANG Hui-yuan, LI Yan-jun. Prominent role of multi-scale microstructural heterogeneities on superplastic deformation of a high solid solution Al−7Mg alloy [J]. International Journal of Plasticity, 2021, 146: 103108.

[80] FURUKAWA M, UTSUNOMIYA A, MATSUBARA K, HORITA Z, LANGDON T G. Influence of magnesium on grain refinement and ductility in a dilute Al−Sc alloy [J]. Acta Materialia, 2001, 49: 3829−3838.

[81] KOMURA S, FURUKAWA M, HORITA Z, NEMOTO M, LANGDON T G. Optimizing the procedure of equal-channel angular pressing for maximum superplasticity [J]. Materials Science and Engineering A, 2001, 297: 111−118.

[82] YUZBEKOVA D, MOGUCHEVA A, KAIBYSHEV R. Superplasticity of ultrafine-grained Al−Mg−Sc−Zr alloy [J]. Materials Science and Engineering A, 2016, 675: 228−242.

[83] MYSHLYAEV M, MIRONOV S, KORZNIKOVA G, KONKOVA T, KORZNIKOVA E, ALETDINOV A, KHALIKOVA G. EBSD study of superplastically strained Al−Mg−Li alloy [J]. Materials Letters, 2020, 275: 128063.

[84] HORITA Z, FURUKAWA M, NEMOTO M, BARNES A J, LANGDON T G. Superplastic forming at high strain rates after severe plastic deformation [J]. Acta Materialia, 2000, 48: 3633−3640.

[85] LEE S, UTSUNOMIYA A, AKAMATSU H, NEISHI K, FURUKAWA M, HORITA Z, LANGDON T G. Influence of scandium and zirconium on grain stability and superplastic ductilities in ultrafine-grained Al−Mg alloys [J]. Acta Materialia, 2002, 50: 553−564.

[86] MÁLEK P, CIESLAR M, ISLAMGALIEV R K. The influence of ECAP temperature on the stability of Al−Zn−Mg−Cu alloy [J]. Journal of Alloys and Compounds, 2004, 378: 237−241.

[87] KYUNG-TAE P, HANG-JAE L, CHONG S L, WON J N, DONG H S. Enhancement of high strain rate superplastic elongation of a modified 5154 Al by subsequent rolling after equal channel angular pressing [J]. Scripta Materialia, 2004, 51: 479−483.

[88] FURUNO K, AKAMATSU H, OH-ISHI K, FURUKAWA M, HORITA Z, LANGDON T G. Microstructural development in equal-channel angular pressing using a 60° die [J]. Acta Materialia, 2004, 52: 2497−2507.

[89] VENKATESWARLU K, GHOSH M, RAY A K, XU Cheng, LANGDON T G. On the feasibility of using a continuous processing technique incorporating a limited strain imposed by ECAP [J]. Materials Science and Engineering A, 2008, 485: 476−480.

[90] AVTOKRATOVA E, SITDIKOV O, MARKUSHEV M, MULYUKOV R. Extraordinary high-strain rate superplasticity of severely deformed Al−Mg−Sc−Zr alloy [J]. Materials Science and Engineering A, 2012, 538: 386−390.

[91] LEE S, FURUKAWA M, HORITA Z, LANGDON T G. Developing a superplastic forming capability in a commercial aluminum alloy without scandium or zirconium additions [J]. Materials Science and Engineering A, 2003, 342: 294−301.

[92] XU Cheng, DIXON W, FURUKAWA M, HORITA Z, LANGDON T G. Developing superplasticity in a spray-cast aluminum 7034 alloy through equal-channel angular pressing [J]. Materials Letters, 2003, 57: 3588−3592.

[93] XU Cheng, FURUKAWA M, HORITA Z, LANGDON T G. Using ECAP to achieve grain refinement, precipitate fragmentation and high strain rate superplasticity in a spray-cast aluminum alloy [J]. Acta Materialia, 2003, 51: 6139−6149.

[94] YAN Ying, QI Yue, CHEN Li-jia, LI Xiao-wu. Strain rate-dependent high temperature compressive deformation characteristics of ultrafine-grained pure aluminum produced by ECAP [J]. Transactions of Nonferrous Metals Society of China, 2016, 26: 966−973.

[95] DAMAVANDI E, NOUROUZI S, RABIEE S M, JAMAATI R. Effect of ECAP on microstructure and tensile properties of A390 aluminum alloy [J]. Transactions of Nonferrous Metals Society of China, 2019, 29: 931−940.

[96] TANG Lei, PENG Xiao-yan, JIANG Fu-qing, LI Yao, XU Guo-fu. Strong and ductile Al−Zn−Mg−Zr alloy obtained by equal angular pressing and subsequent aging [J]. Transactions of Nonferrous Metals Society of China, 2022, 32: 1428−1441.

[97] BALL A, HUTCHISON M M. Superplasticity in the aluminium-zinc eutectoid [J]. Metal Science Journal, 1969, 3: 1−7.

[98] ASHBY M F, VERRALL R A. Diffusion-accommodated flow and superplasticity [J]. Acta Metall, 1973, 21: 149−163.

[99] GIFKINS R C. Grain-boundary sliding and its accommodation during creep and superplasticity [J]. Metallurgical Transactions A, 1976, 7: 1225−1232.

[100] SOTOUDEH K, BATE P S. Diffusion creep and superplasticity in aluminium alloys [J]. Acta Materialia, 2010, 58: 1909−1920.

[101] MIKHAYLOVSKAYA A V, YAKOVTSEVA O A, GOLOVIN I S, POZDNIAKOV A V, PORTNOY V K. Superplastic deformation mechanisms in fine-grained Al−Mg based alloys [J]. Materials Science and Engineering A, 2015, 627: 31−41.

[102] LI Guang-yu, DING Hua, ZHANG Yu. Surface studies of superplasticity in A−Zn−Mg−Cu alloy via in-situ tensile test [J]. Materials Science and Engineering A, 2022, 841: 142930.

[103] LIU Xiao-dong, YE Ling-ying, TANG Jian-guo, KE Bin, DONG Yu, CHEN Xiao-jiao, GU Yi. Superplastic deformation mechanisms of a fine-grained Al−Cu−Li alloy [J]. Materials Science and Engineering A, 2022, 848: 143403.

[104] PEARSON C E. The viscous properties of extruded eutectic alloys of lead−tin and bismuth−tin [J]. J Inst Materials, 1934, 54: 111−124.

[105] BACKOFEN W A. Superplasticity in an Al−Zn alloy [J]. Trans ASM, 1964, 57: 980−990.

[106] LARRY D H. Commercial airplane applications of superplastically formed AA5083 aluminum sheet [J]. Journal of Materials Engineering and Performance, 2007, 16: 136−141.

[107] BARNES A J. Industrial applications of superplastic forming: Trends and prospects [J]. Materials Science Forum, 2001, 357/358/359: 3−16.

[108] VYSOTSKIY I, KIM K, MALOPHEYEV S, MIRONOV S, KAIBYSHEV R. Superplastic behavior of friction-stir welded Al−Mg−Sc−Zr alloy in ultrafine-grained condition [J]. Transactions of Nonferrous Metals Society of China, 2022, 32: 1083−1095.

[109] NIEH T G, WADSWORTH J, SHERBY O D. Superplasticity in metals and ceramics [M]. Cambridge: Cambridge University Press, 1997.

[110] LIU Zhan, NIE Jin-feng, ZHAO Yong-hao. Effect of deformation processing on microstructure evolution and mechanical properties of Mg−Li alloys: A review [J]. Transactions of Nonferrous Metals Society of China, 2024, 34: 1−25.

[111] ALABORT E, PUTMAN D, REED R C. Superplasticity in Ti−6Al−4V: Characterisation, modelling and applications [J]. Acta Materialia, 2015, 95: 428−442.

[112] PRATYUSH A S, OMIHIR O, LAKSHMAN R K, KUMAR G A. A review on superplastic forming of Ti−6Al−4V and other titanium alloys [J]. Materials Today Communications, 2023, 34: 105343.

[113] YANG Jun-zhou, WU Jian-jun, XIE Hai-nan, LI Zhi-guo, WANG Kai-wei. Mechanism of continuous dynamic recrystallization of Ti−6Al−4V alloy during superplastic forming with sub-grain rotation [J]. Transactions of Nonferrous Metals Society of China, 2023, 33: 777−788.

[114] MIRACLE D B, SENKOV O N. A critical review of high entropy alloys and related concepts [J]. Acta Materialia, 2017, 122: 448−511.

[115] SOHRABI M J, KALHOR A, MIRZADEH H, RODAK K, KIM H S. Tailoring the strengthening mechanisms of high-entropy alloys toward excellent strength-ductility synergy by metalloid silicon alloying: A review [J]. Progress in Materials Science, 2024, 144: 101295.

[116] ZHANG Pan, YE Ling-ying, ZHANG Xin-ming, GU Gang, JIANG Hai-chun, WU Yu-long. Grain structure and microtexture evolution during superplastic deformation of 5A90 Al−Li alloy [J]. Transactions of Nonferrous Metals Society of China, 2014, 24: 2088−2093.

[117] MALOPHEYEV S, MIRONOV S, VYSOTSKIY I, KAIBYSHEV R. Superplasticity of friction-stir welded Al−Mg−Sc sheets with ultrafine-grained microstructure [J]. Materials Science and Engineering A, 2016, 649: 85−92.

[118] HASLAM A J, MOLDOVAN D, YAMAKOV V, WOLF D, PHILLPOT S R, GLEITER H. Stress-enhanced grain growth

in a nanocrystalline material by molecular-dynamics simulation [J]. Acta Materialia, 2003, 51: 2097−2112.

[119] MASUDA H, KANAZAWA T, TOBE H, SATO E. Dynamic anisotropic grain growth during superplasticity in Al−Mg−Mn alloy [J]. Scripta Materialia, 2018, 149: 84−87.

[120] NES E. Hot deformation behaviour of particle-stabilized structures in Zr-bearing Al alloys [J]. Metal Science, 2013, 13: 211−215.

[121] KAIBYSHEV R, AVTOKRATOVA E, APOLLONOV A, DAVIES R. High strain rate superplasticity in an Al−Mg−Sc−Zr alloy subjected to simple thermomechanical processing [J]. Scripta Materialia, 2006, 54: 2119−2124.

[122] DENG Ying, YIN Zhi-min, PAN Qin-lin, XU Guo-fu, DUAN Yu-lu, WANG Ying-jun. Nano-structure evolution of secondary $Al_3(Sc_{1-x}Zr_x)$ particles during superplastic deformation and their effects on deformation mechanism in Al−Zn−Mg alloys [J]. Journal of Alloys and Compounds, 2017, 695: 142−153.

[123] MOCHUGOVSKIY A G, MIKHAYLOVSKAYA A V, TABACHKOVA N Y, PORTNOY V K. The mechanism of L12 phase precipitation, microstructure and tensile properties of Al−Mg−Er−Zr alloy [J]. Materials Science and Engineering A, 2019, 744: 195−205.

[124] MAENG D Y, LEE J. H, HONG S I. The effect of transition elements on the superplastic behavior of Al−Mg alloys [J]. Materials Science and Engineering A, 2003, 357: 188−195.

[125] LIU Xiao-dong, YE Ling-ying, TANG Jian-guo, SHAN Zhao-jun, KE Bin, DONG Yu, CHEN Jin. Superplastic deformation mechanisms of an Al−Mg−Li alloy with banded microstructures [J]. Materials Science and Engineering A, 2021, 805: 140545.

[126] HUMPHREYS F J. Local lattice rotations at second phase particles in deformed metals [J]. Acta Metallurgica, 1979, 27: 1801−1814.

[127] HUMPHREYS F J. The nucleation of recrystallization at second phase particles in deformed aluminium [J]. Acta Metallurgica, 1977, 25: 1323−1344.

[128] SHEN Jiao-jiao, CHEN Biao, WAN Jie, SHEN Jiang-hua, LI Jin-shan. Effect of annealing on microstructure and mechanical properties of an Al−Mg−Sc−Zr alloy [J]. Materials Science and Engineering A, 2022, 838: 142821.

[129] LI Qun, NING Jian, CHEN Lei, HU Jian-liang, LIU Yuan-xi. The mechanical response and microstructural evolution of 2195 Al−Li alloy during hot tensile deformation [J]. Journal of Alloys and Compounds, 2020, 848: 156515.

[130] CHOKSHI A H. Cavity nucleation and growth in superplasticity [J]. Materials Science and Engineering A, 2005, 410/411: 95−99.

[131] LIN Zhao-rong, CHOKSHI A H, LANGDON T G. An investigation of grain boundary sliding in superplasticity at high elongations [J]. Journal of Materials Science 1988, 23: 2712−2722.

[132] CAO Fu-rong, LI Zhuo-liang, ZHANG Nian-xian, DING Hua, YU Fu-xiao, ZUO Liang. Superplasticity, flow and fracture mechanism in an Al−12.7Si−0.7Mg alloy [J]. Materials Science and Engineering A, 2013, 571: 167−183.

[133] BAE D H, GHOSH A K. Grain size and temperature dependence of superplastic deformation in an Al−Mg alloy under isostructural condition [J]. Acta Materialia, 2000, 48: 1207−1224.

[134] MOHAMED F A, AHMED M M I, LANGDON T G. Factors influencing ductility in the superplastic Zn−22%Al eutectoid [J]. Metallurgical Transactions A, 1977, 8: 933−938.

[135] PILLING J, RIDLEY N. Superplasticity in crystalline solids [J]. The Institute of Metals, 1989: 102−158.

[136] YAKOVTSEVA O A, KISHCHIK A A, CHEVERIKIN V V, KOTOV A D, MIKHAYLOVSKAYA A V. The mechanisms of the high-strain-rate superplastic deformation of Al−Mg-based alloy [J]. Materials Letters, 2022, 325: 132883.

[137] MCNELLEY T R, OH-ISHI K, ZHILYAEV A P, SWAMINATHAN S, KRAJEWSKI P E., TALEFF E M. Characteristics of the transition from grain-boundary sliding to solute drag creep in superplastic AA5083 [J]. Metallurgical and Materials Transactions A, 2007, 39: 50−64.

[138] DUAN Yu-lu, QIAN Jian, XIAO Dan, CUI Xue-min, XU Guo-fu. Effect of Sc and Er additions on superplastic ductilities in Al−Mg−Mn−Zr alloy [J]. Journal of Central South University, 2016, 23: 1283−1292.

[139] BI S, LIU Z Y, YU B H, MA G N, WU L H, XIAO B L, MA Z Y. Superplastic deformation behavior of carbon nanotube reinforced 7055 Al alloy composites [J]. Materials Science and Engineering A, 2020, 797: 140263.

[140] LI Meng-jia, PAN Qing-lin, SHI Yun-jia, SUN Xue, XIANG Hao. High strain rate superplasticity in an Al−Mg−Sc−Zr alloy processed via simple rolling [J]. Materials Science and Engineering A, 2017, 687: 298−305.

[141] HOTZ W, RUEDL E, SCHILLER P. Observation of processes of superplasticity with the scanning electron microscope [J]. Journal of Materials Science, 1975, 10: 2003−2006.

[142] VALIEV R Z, LANGDON T G. An investigation of the role of intragranular dislocation strain in the superplastic Pb−62%Sn eutectic alloy [J]. Acta Metallurgica et Materialia, 1993, 41: 949−954.

[143] LI P, CHEN S, DAI H, YANG Z, CHEN Z, WANG Y, CHEN Y, PENG W, SHAN W, DUAN H. Recent advances in focused ion beam nanofabrication for nanostructures and devices: Fundamentals and applications [J]. Nanoscale, 2021, 13: 1529−1565.

[144] RUST M A, TODD R I. High resolution surface studies of superplastic deformation in shear and tension [J]. Materialwissenschaft und Werkstofftechnik, 2008, 39: 289−292.

[145] LI Jun, YE Ling-ying, LIU Xiao-dong, DONG Yu. In-situ surface study of the mechanism of high temperature deformation in an Al−Cu−Li alloy [J]. Materials Letters, 2023, 336: 133889.

[146] MIKHAYLOVSKAYA A V, YAKOVTSEVA O V, SITKINA M N, KOTOV A D. Grain-boundary and intragranular deformation in ultrafine-grained aluminum-based alloy at high strain rate [J]. Materials Letters, 2020, 276: 128242.

[147] YAKOVTSEVA O A, TOMAS A, MIKHAYLOVSKAYA A. Surface and internal structural markers for studying grain boundary sliding and grain rotation [J]. Materials Letters, 2020, 268: 127569.

[148] YAKOVTSEVA O A, SITKINA M N, KOTOV A D, ROFMAN O V, MIKHAYLOVSKAYA A V. Experimental study of the superplastic deformation mechanisms of high-strength aluminum-based alloy [J]. Materials Science and Engineering A, 2020, 788.
[149] MIKHAYLOVSKAYA A V, YAKOVTSEVA O A, SITKINA M N, KOTOV A D, IRZHAK A V, KRYMSKIY S V, PORTNOY V K. Comparison between superplastic deformation mechanisms at primary and steady stages of the fine grain AA7475 aluminium alloy [J]. Materials Science and Engineering A, 2018, 718: 277−286.
[150] RUST M A, TODD R I. Surface studies of region II superplasticity of AA5083 in shear: Confirmation of diffusion creep, grain neighbour switching and absence of dislocation activity [J]. Acta Materialia, 2011, 59: 5159−5170.
[151] PORTNOY V K, NOVIKOV I I. Evaluation of grain boundary sliding contribution to the total strain during superplastic deformation [J]. Scripta Materialia, 1998, 40: 39−43.

超塑性铝合金的显微组织演变及变形机理综述

邹国童[1]，陈世杰[1]，徐亚琪[1]，沈保坤[1]，张瑜佳[1]，叶凌英[1,2,3]

1. 中南大学 材料科学与工程学院，长沙 410083；
2. 中南大学 有色金属科学与工程教育部重点实验室，长沙 410083；
3. 中南大学 有色金属先进结构材料与制造协同创新中心，长沙 410083

摘　要：铝合金是最早开始使用且应用最广泛的超塑性材料之一。综述了超塑性铝合金的研究进展，重点总结了铝合金在超塑性变形过程中的显微组织演变和变形机理，详细讨论了典型超塑性铝合金在超塑性变形过程中晶粒组织、织构、第二相和空洞的演变。基于聚焦离子束(FIB)的表面研究能为不同超塑性变形机制提供定量评估，从而为研究铝合金的超塑性提供新的思路。基于 FIB 的表面研究可以直观地观察到晶界滑移、晶内位错滑移和扩散蠕变等主要特征，并进行定量分析。本研究可为超塑性变形机理的研究和超塑性铝合金的发展提供一定的参考。

关键词：铝合金；超塑性；超塑性变形机理；晶界滑移；显微组织演变

(Edited by Bing YANG)